NATIONAL ENERGY TECHNOLOGY LABORATORY

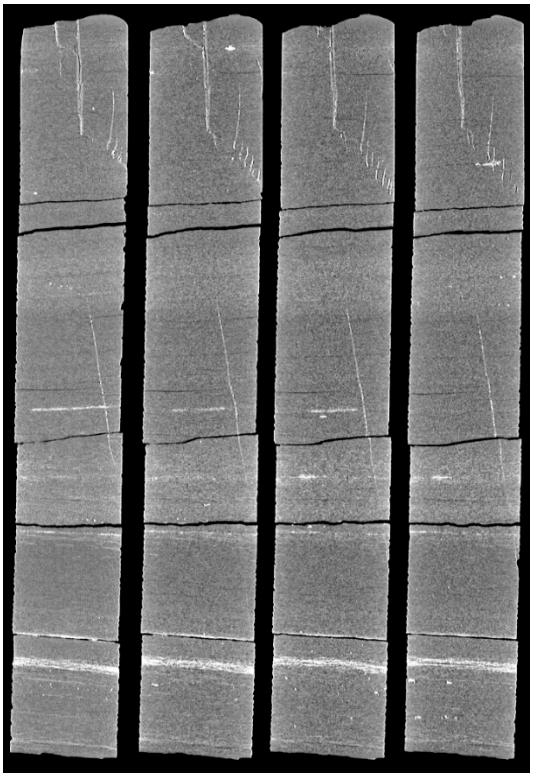

Computed Tomography Scanning and Geophysical Measurements of the Marcellus Formation from the Armstrong #1 Well

X September 2018

Preliminary – Do not cite or quote

U.S. DEPARTMENT OF ENERGY | NATIONAL ENERGY TECHNOLOGY LABORATORY

Office of Fossil Energy

NETL-TRS-X-2018

Disclaimer

Cover Illustration: Montage of computed tomography scans through Armstrong #1 well core from a depth of ~7,700 to 7,702 ft. Images show mineral filled fractures within the core and are 10.75 mm apart.

Suggested Citation: Paronish, T.; Mackey, P.; Crandall, D.; Moore, J.; Brown, S.; Carr, T.; Dinterman, P; Jarvis, K. *Computed Tomography Scanning and Geophysical Measurements of the Marcellus Formation from the Armstrong #1 Well;* NETL-TRS-X-2018; NETL Technical Report Series; U.S. Department of Energy, National Energy Technology Laboratory: Morgantown, WV, 2018; p XX.

An electronic version of this report can be found at:

http://netl.doe.gov/research/on-site-research/publications/featured-technical-reports

https://edx.netl.doe.gov/ucr

The data in this report can be accessed from NETL's Energy Data eXchange (EDX) online system (https://edx.netl.doe.gov) using the following link: https://edx.netl.doe.gov/dataset/armstrong-well

Computed Tomography Scanning and Geophysical Measurements of the Marcellus Formation from the Armstrong #1 Well

Thomas Paronish[1,2], Paige Mackey[1,2], Dustin Crandall[1], Johnathan Moore[1,3], Sarah Brown[1,3], Tim Carr[4], Phillip Dinterman[5], Karl Jarvis[1,3]

[1]U.S. Department of Energy, National Energy Technology Laboratory, 3610 Collins Ferry Road, Morgantown, WV 26507

[2]U.S. Department of Energy, National Energy Technology Laboratory, ORISE, 3610 Collins Ferry Road, Morgantown, WV 26507

[3]U.S. Department of Energy, National Energy Technology Laboratory, AECOM, 3610 Collins Ferry Road, Morgantown, WV 26507

[4]West Virginia University, Department of Geology and Geography, 98 Beechurst Avenue, Morgantown, WV 26506

[5]West Virginia Geological and Economic Survey, 1 Mont Chateau Road, Morgantown, WV 26508

NETL-TRS-X-2018

X September 2018

NETL Contacts:

Dustin Crandall, Principal Investigator

Alexandra Hakala, Technical Portfolio Lead

Bryan Morreale, Executive Director, Research & Innovation Center

This page intentionally left blank.

Table of Contents

This page intentionally left blank.

List of Figures

List of Figures (cont.)

List of Tables

Acronyms, Abbreviations, and Symbols

Term	Description
2D	Two-dimensional
3D	Three-dimensional
CT	Computed tomography
EDX	NETL's Energy Data eXchange
EIA	U.S. Energy Information Administration
MSCL	Multi-Sensor Core Logger
NETL	National Energy Technology Laboratory
WVGES	West Virginia Geological and Economic Survey
WVU	West Virginia University
XRF	X-ray fluorescence

Acknowledgments

This work was completed at the National Energy Technology Laboratory (NETL) with support from U.S. Department of Energy's (DOE) Office of Fossil Energy Oil & Gas Program. The authors wish to acknowledge Bryan Morreale and Alexandra Hakala (NETL Research & Innovation Center), Jared Ciferno, (NETL Technology Development and Integration Center), and Elena Melchert (DOE Office of Fossil Energy) for programmatic guidance, direction, and support.

The authors would like to thank Bryan Tennant, Scott Workman, and Roger Lapeer for data collection and technical support. Thank you to Petroleum Development Corporation for allowing us to work with this core. Thank you to Kelly Rose, Dustin McIntyre, and Mark McKoy for laboratory support. This research was supported in part by appointments from the NETL Research Participation Program, sponsored by the U.S. DOE and administered by the Oak Ridge Institute for Science and Education (ORISE).

ABSTRACT

The computed tomography (CT) facilities and the Multi-Sensor Core Logger (MSCL) at the National Energy Technology Laboratory (NETL) in Morgantown, West Virginia were used to characterize core from the Marcellus Formation. The core is from a vertical well (Armstrong #1) drilled in Taylor County, West Virginia by the Petroleum Development Corporation (7,545 to 7,783.4 ft). Core was provided by Phillip Dinterman, West Virginia Geologic and Economical Survey (WVGES) and Tim Carr and Keithan Martin, West Virginia University (WVU).

The primary impetus of this work is a collaboration between NETL, WVGES, and WVU to characterize core from multiple wells to better understand the structure and variation of the Marcellus and Utica Shale formations. As part of this effort, bulk scans of core were obtained from the Armstrong #1 well. This report, and the associated scans, provide detailed datasets not typically available from unconventional shales for analysis. The resultant datasets are presented in this report, and can be accessed from NETL's Energy Data eXchange (EDX) online system using the following link: https://edx.netl.doe.gov/dataset/armstrong-well.

All equipment and techniques used were non-destructive, enabling future examinations and analyses to be performed on these cores. None of the equipment used was suitable for direct visualization of the shale pore space, although fractures and discontinuities were detectable with the methods tested. Low resolution CT imagery with the NETL medical CT scanner was performed on the entire core. Qualitative analysis of the medical CT images, coupled with X-ray fluorescence (XRF), P-wave, and magnetic susceptibility measurements from the MSCL were useful in identifying zones of interest for more detailed analysis as well as fractured zones. The ability to quickly identify key areas for more detailed study with higher resolution will save time and resources in future studies. The combination of methods used provides a multi-scale analysis of the core; the resulting macro and micro descriptions are relevant to many subsurface energy related examinations traditionally performed at NETL.

1. INTRODUCTION

Evaluation of reservoir samples can support resource estimation and determination of effective extraction methodologies. While it is common for commercial entities to perform these characterizations, the resources necessary to conduct these analyses are not always available to the broader interest base, such as state agencies and research-based consortiums. To meet the growing need for comprehensive and high-quality lithologic data for collaborative research initiatives, the National Energy Technology Laboratory (NETL) has used available resources in conjunction with previous techniques and new, innovative methodologies to develop a systematic approach for the evaluation of cores. In this report, data collected from a Marcellus Shale production wildcat well in Taylor County, West Virginia are presented as one part of a broader collaborative effort by West Virginia Geologic and Economical Survey (WVGES), West Virginia University (WVU), and NETL to better characterize this important, spatially heterogeneous, formation.

In this study, the primary objective was to characterize core from depth with methods not available to most researchers. The data is presented in several formats here and online that are potentially useful for various analyses, however, little detailed analysis is presented in this report as the research objective was not to do a site characterization, but rather to develop the data for others to utilize and to create a digital representation of the core that could be preserved.

The core described here is from the wildcat Armstrong #1 well that was completed in 2009 (API No: 47-091-01116); the geographic coordinates for the well are: latitude 39.291926 N, longitude -80.08322 W (Figures 1 and 2). The well pad elevation was 1,331 ft. As shown in Figures 1 and 2, the Marcellus in this area is expected to be approximately 100 to 150 ft thick and appear at a depth of 6,000 and 7,000 ft below sea level.

As part of this collaboration to characterize core from multiple wells and better understand the structure and variation of the Marcellus and Utica shale formations, bulk scans of core were performed using fast scanning techniques to obtain base-line information on sample condition and characteristics. For similar measurements from nearby wells through the Marcellus Shale formation in Pennsylvania and Ohio, please see Crandall et al. (2018a,b).

Table 1: Core box distribution Armstrong #1 well as received

	Number of Boxes	Depth Range (ft)
Core 1	21	7,545–7,605.5
Core 2	21	7,605.5–7,666
Core 3	20	7,666.3–7,724.6
Core 4	20	7,724.6–7,783.4

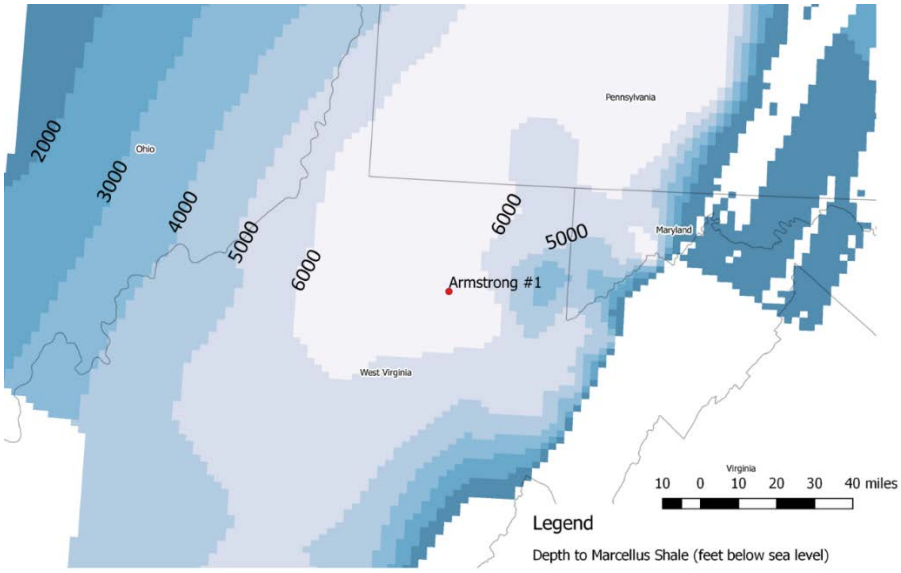

Figure 1: Armstrong location map including depths to the Marcellus Formation boundary (ft below sea level) from the U.S. Energy Information Administration (EIA, 2018).

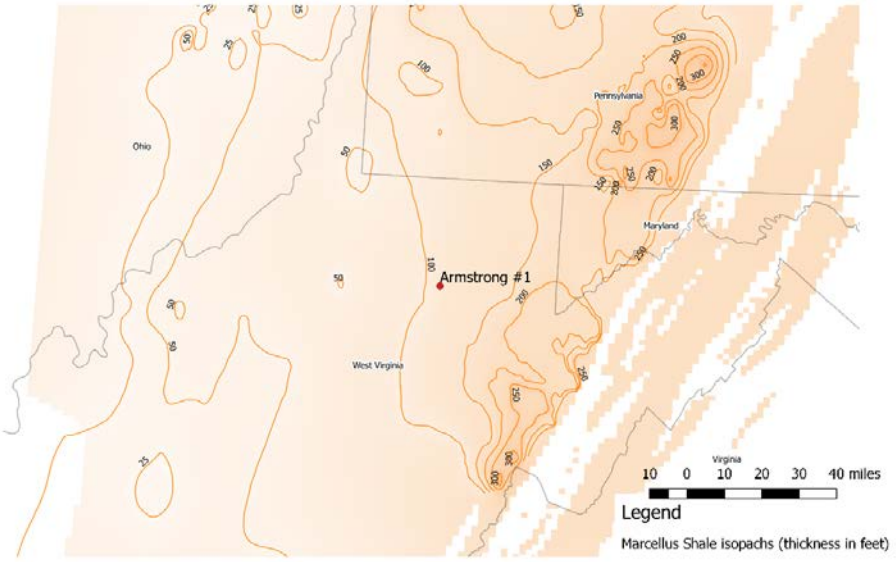

Figure 2: Armstrong location map including isopach contours of the Marcellus Shale (ft) from the U.S. Energy Information Administration (EIA, 2018).

2. CORE DESCRIPTION

The core lithology consists of medium dark-gray to dark-gray, clay-rich shale, which transitions into dark-gray to black, siliceous, organic-rich shale, becoming calcareous and fossil-rich at the base of the cored interval. Fine to medium silt-sized quartz and mica are present with minor calcite cement and some pyrite replacement. Concretions are present including: barite and siderite concretions within the Mahantango (7,545 to 7,675 ft) and calcite with minor pyrite replacement within the Marcellus (7,675 to 7,800.5 ft). The missing sections were sub-sampled at earlier times or consist of rubble zones. Table 2 lists the abbreviations used in the descriptions in the detailed lithology log presented in Figure 3.

Table 2: Abbreviations used in the detailed lithology log in Figure 3

Term	Description
bl	black
cal	calcareous
dbr-bl	dark brown to black
dg	dark gray
dg-bl	dark gray to black
fg	fine-grained
fz	fracture zone
fz dg-bl	fracture zone dark gray to black
fz mdg-dg	fracture zone medium dark gray to dark gray
ls	limestone
lg	light gray
mdg	medium dark gray
mdg-dg	medium dark gray to dark gray
pyr	pyrite
rz	rubble zone
rz mdg-dg	rubble zone medium dark gray to dark gray
sh	shale
vert	vertical

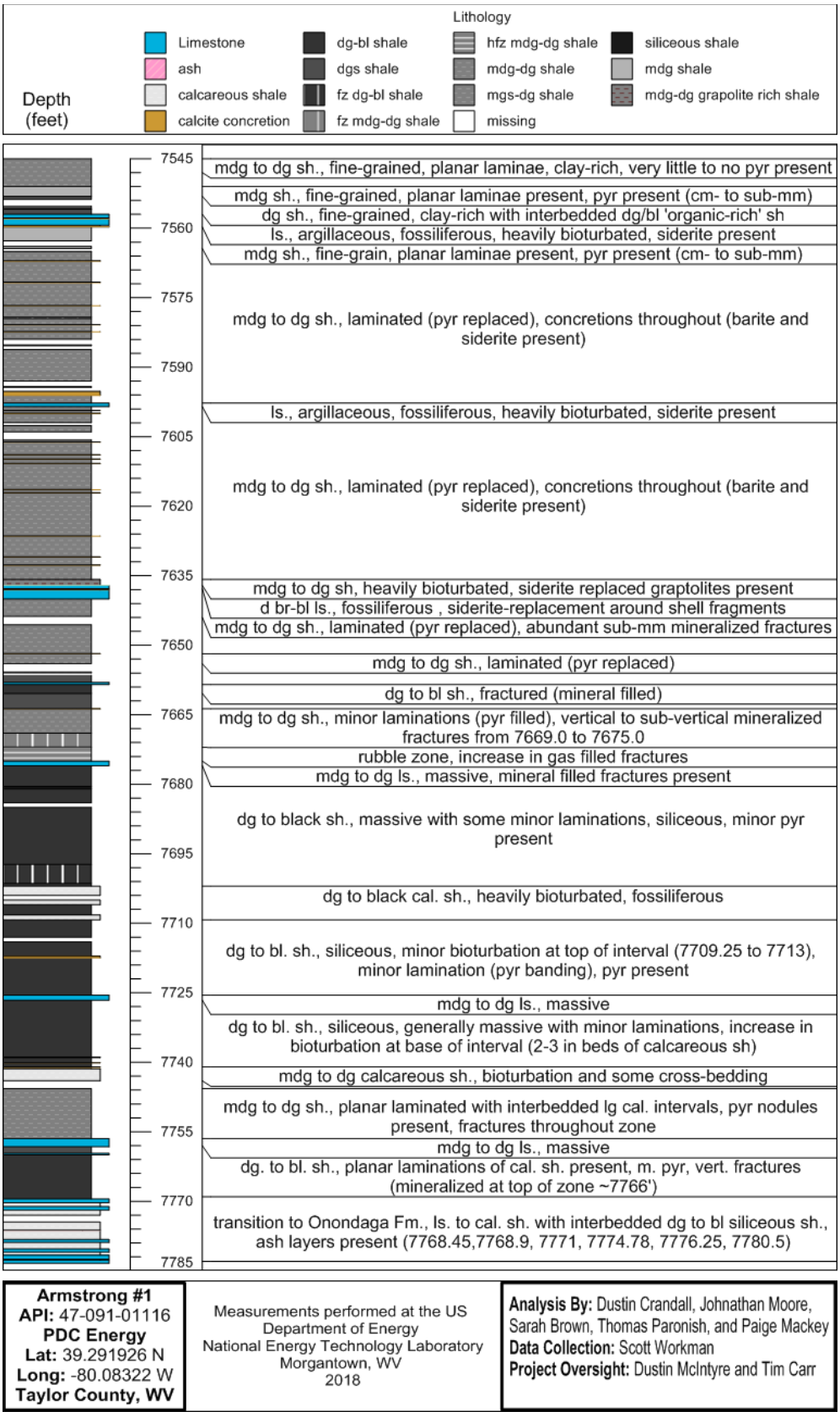

Figure 3: Detailed core description for Armstrong #1 from 7,545 to 7,783.4 ft.

2.1 CORE PHOTOGRAPHS

Photographs of the 2/3 slabbed core.

Figure 4: Armstrong #1 core photographs, from 7,545 to 7,562.75 ft.

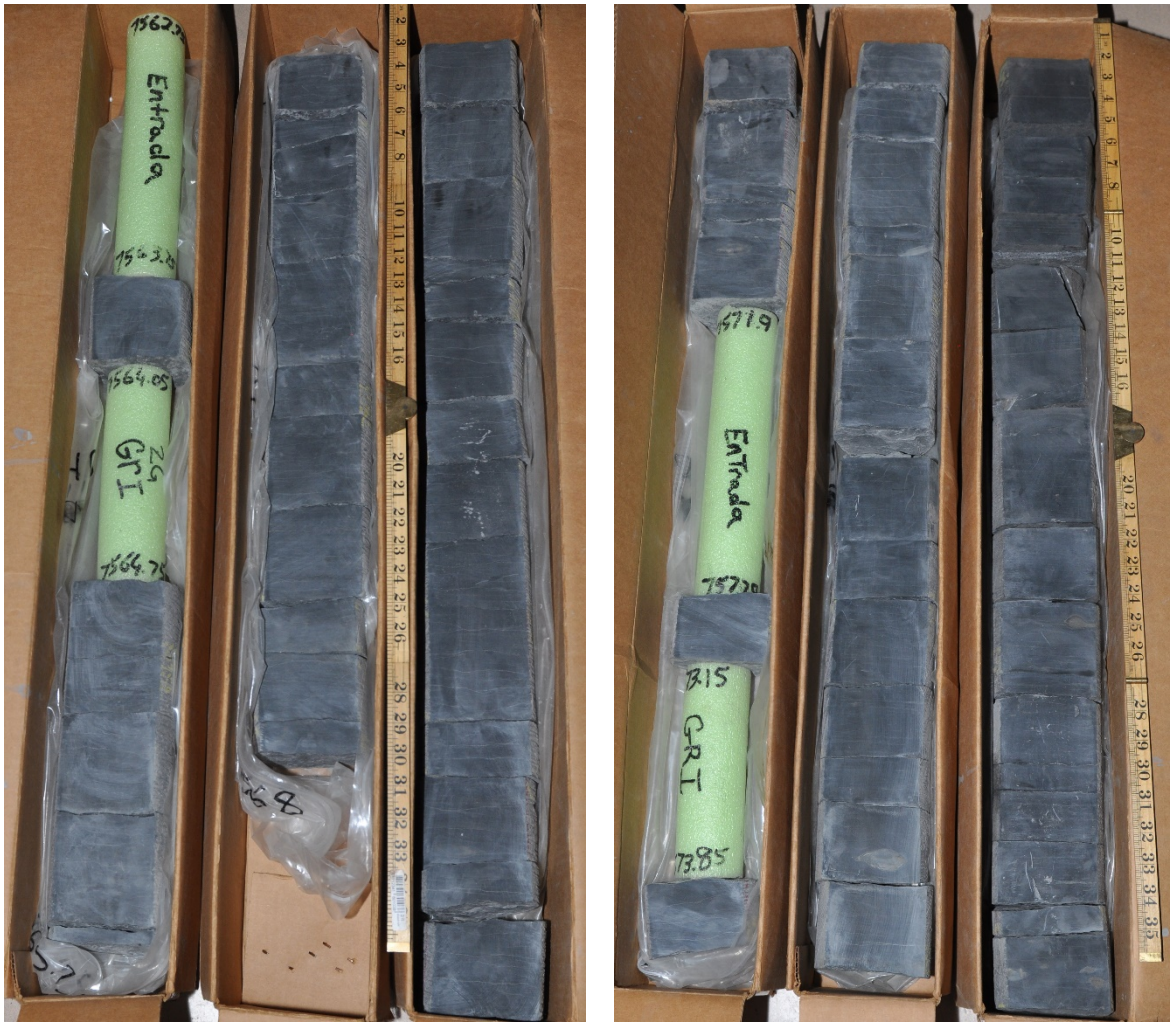

Figure 5: Armstrong #1 core photographs, from 7,562.75 to 7,580 ft.

Figure 6: Armstrong #1 core photographs, from 7,580 to 7,598 ft.

Figure 7: Armstrong #1 core photographs, from 7,598 to 7,612 ft.

Figure 8: Armstrong #1 core photographs, from 7,612 to 7,630 ft.

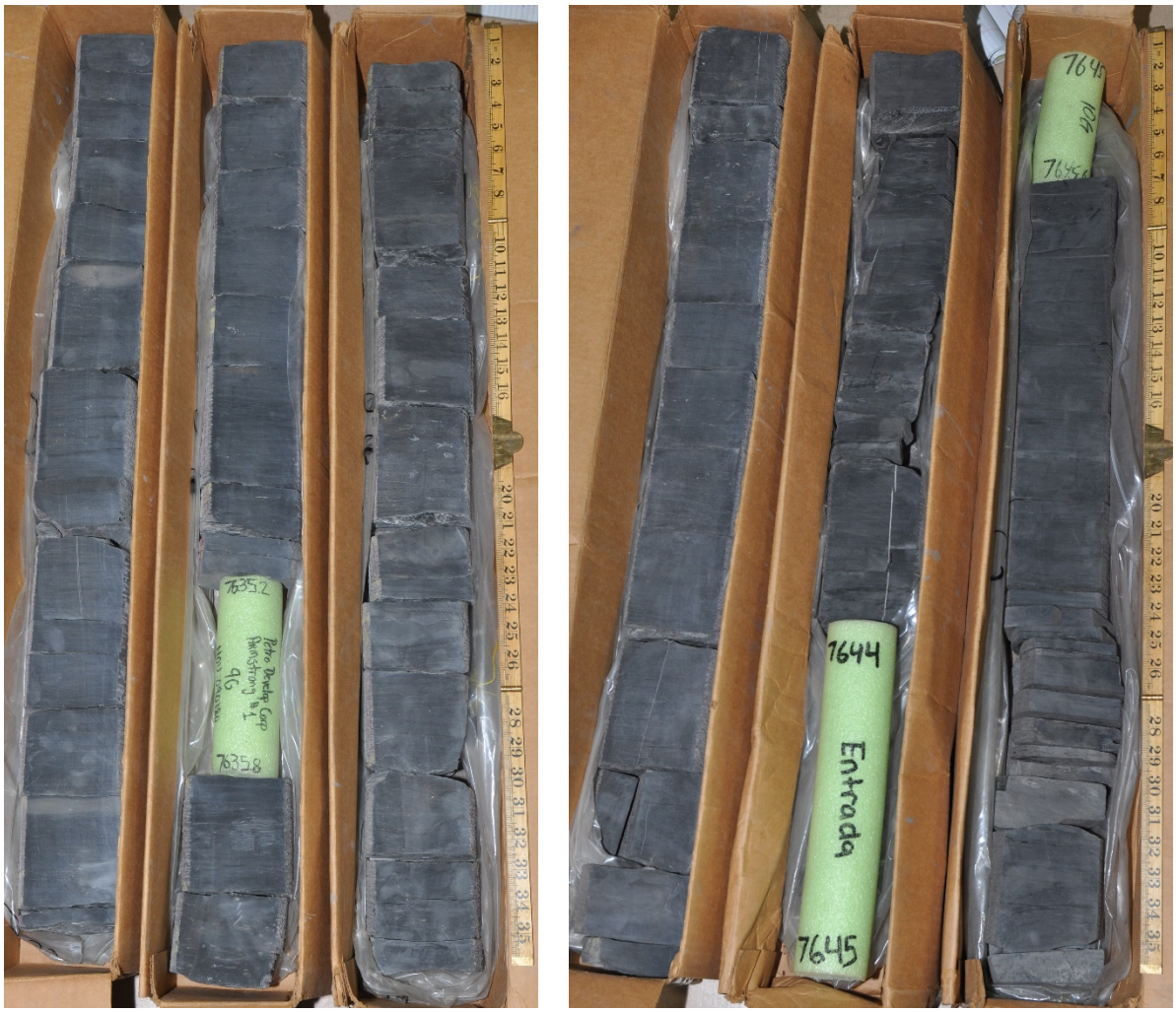

Figure 9: Armstrong #1 core photographs, from 7,630 to 7,648 ft.

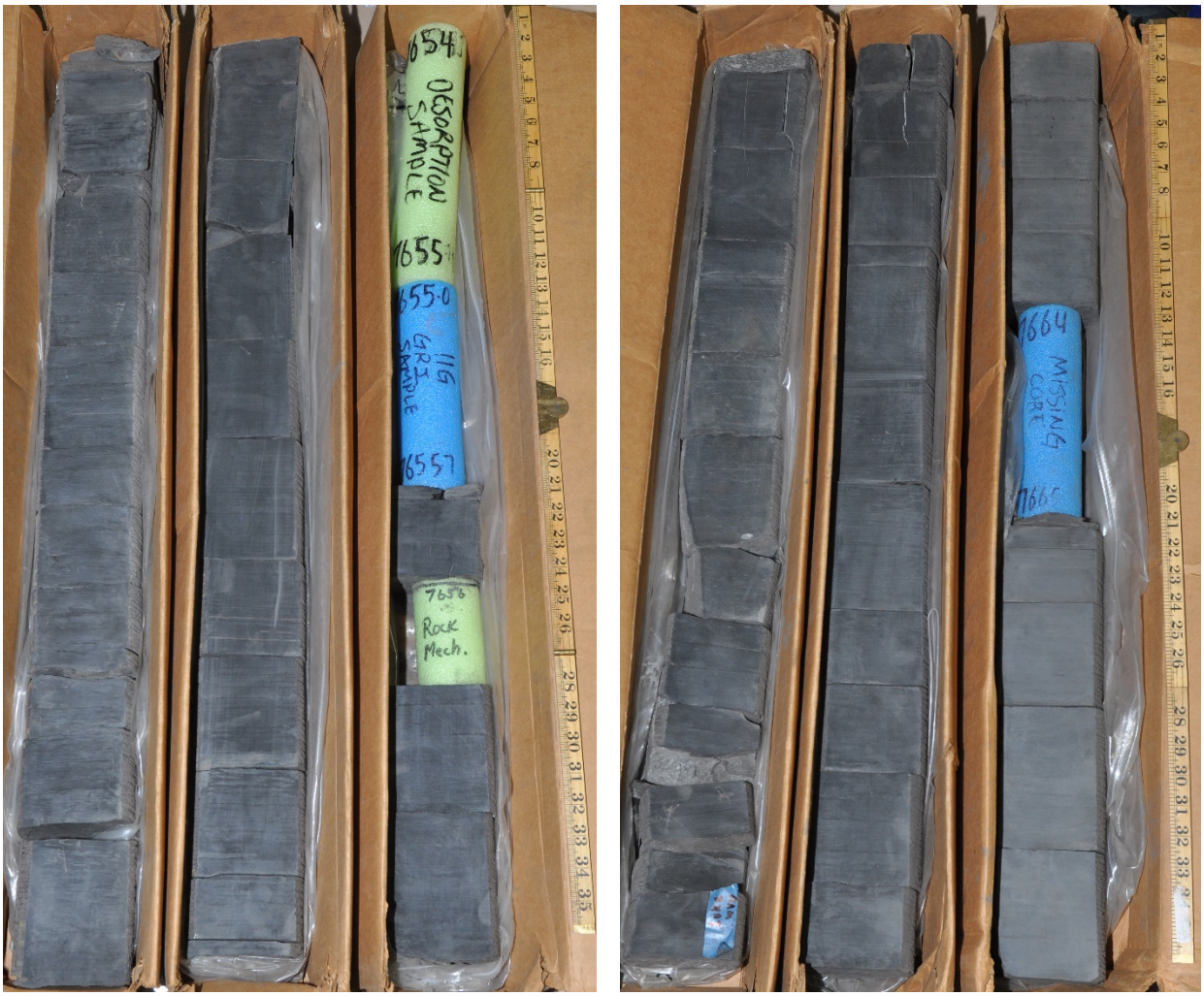

Figure 10: Armstrong #1 core photographs, from 7,648 to 7,666 ft.

Figure 11: Armstrong #1 core photographs, from 7,666.3 to 7,684 ft.

Figure 12: Armstrong #1 core photographs, from 7,684 to 7,702 ft.

Figure 13: Armstrong #1 core photographs, from 7,702 to 7,720 ft.

Figure 14: Armstrong #1 core photographs, from 7,720 to 7,732.9 ft.

Figure 15: Armstrong #1 core photographs, from 7,732.9 to 7,751 ft.

Figure 16: Armstrong #1 core photographs, from 7,751 to 7,769 ft.

Figure 17: Armstrong #1 core photographs, from 7,769 to 7,783.4 ft.

Figure 18: Detailed images of en echelon fractures at depths from 7,670 to 7,672 ft.

Mineralized en echelon fractures (Figure 18) indicate the presence of shear stress and can be used to gain insight into local variations on the regional stress field or deformation history. Changes in fracture structure could be caused by changes in mineral composition of the surrounding matrix, that has been shown to contribute to the brittleness of shales (Jarvie et al., 2007; Wang and Gale, 2009). The effectiveness of hydraulic stimulations are controlled, in part, by the brittleness of shale.

3. DATA ACQUISITION AND METHODOLOGY

The 2/3 slabbed core was evaluated using computed tomography (CT) scanning and traditional core logging.

3.1 CORE LOGGING

Geophysical measurements of core thickness deviation, P-wave travel time, magnetic susceptibility, and attenuated gamma counts can be obtained with a Geotek® Multi-Sensor Core Logging (MSCL, Figure 19) system on a competent section of core. For the 2/3 slabbed core that was scanned as part of this analysis the P-wave velocity were measured and reported. Additionally, the system was used to measure bulk elemental chemistry with a built-in, portable X-ray fluorescence (XRF) spectrometer. For a full description of the MSCL capabilities at NETL, please see Crandall et al. (2017).

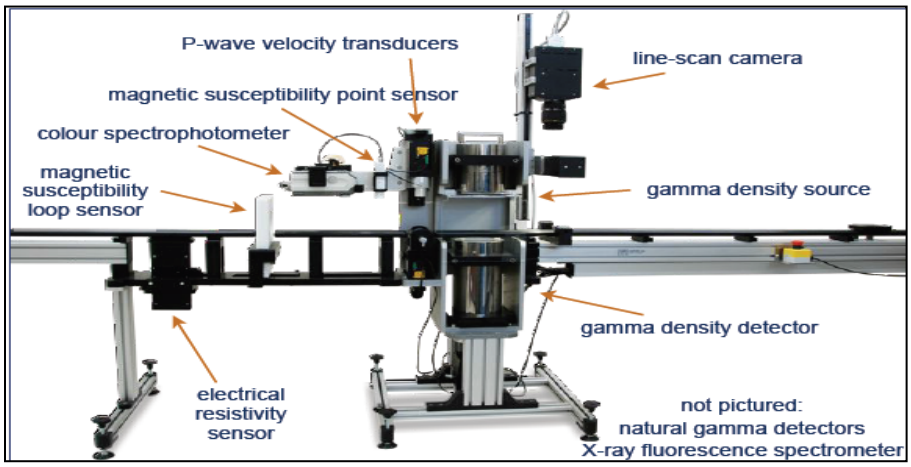

Figure 19: Representation of generalized MSCL with all attached instruments. From Geotek Ltd., Geotek Multi-Sensor Core Logger Flyer, Daventry, UK (2009).

3.1.1 Magnetic Susceptibility

Magnetic susceptibility is a measure of the degree of magnetization in a sample. The sample is passed through a ring apparatus with an oscillating magnetic field, where the interference to this field is proportional to the magnetism of the sample, and thus a relative measurement can be taken. The measurement unit used is dimensionless (abbreviated simply as SI units) and is based on the original calibration, which is done via stable iron oxides, and reference minerals which have known ranges of susceptibility (Table 3) (Geotek Ltd. Multi-Sensor Core Logger Manual, Version 05-10).

Table 3: Magnetic susceptibility values for common minerals (Modified from Geotek Ltd. Multi-Sensor Core Logger Manual, Version 05-10, 2010)

Mineral	X (*10^{-6}) SI
Water	9
Calcite	-7.5 to -39
Halite, Gypsum	-10 to -60
Illite, Montmorillonite	330 to 410
Pyrite	5 to 3,500
Haematite	500 to 40,000
Magnetite	1,000,000 to 5,700,000

3.1.2 P-wave Velocity

P-wave velocity measurements are performed to measure the acoustic impedance of a geologic sample with compressional waves. Acoustic impedance is a measure of how well a material transmits vibrations, which is directly proportional to density and/or material consolidation. An example of a material that has a high acoustic impedance would be air, with a wave speed of 330 m/s, whereas granite would have low acoustic impedance, with a wave speed of >5,000 m/s. These measurements can be proxies for seismic reflection coefficients and can be translated to field use when during seismic surveys.

The software associated with the MSCL measures the travel time of the pulse with a resolution of 50 ns. The absolute accuracy of the instrument measurements is $\pm$ 3 m/s with a resolution of 1.5 m/s (Geotek Ltd. Multi-Sensor Core Logger Manual, Version 05-10; Geotek Ltd., 2010).

3.1.3 X-ray Fluorescence Spectrometry

In addition to the geophysical measurements a portable handheld Delta Standard Innov-X® X-Ray Fluorescence Spectrometer was used to measure relative elemental abundances of aggregated “light elements” up to and including sodium, and also various heavy elements which were measured individually (Figure 20). Elemental abundances are reported relative to the total elemental composition, i.e. out of 100% weight.

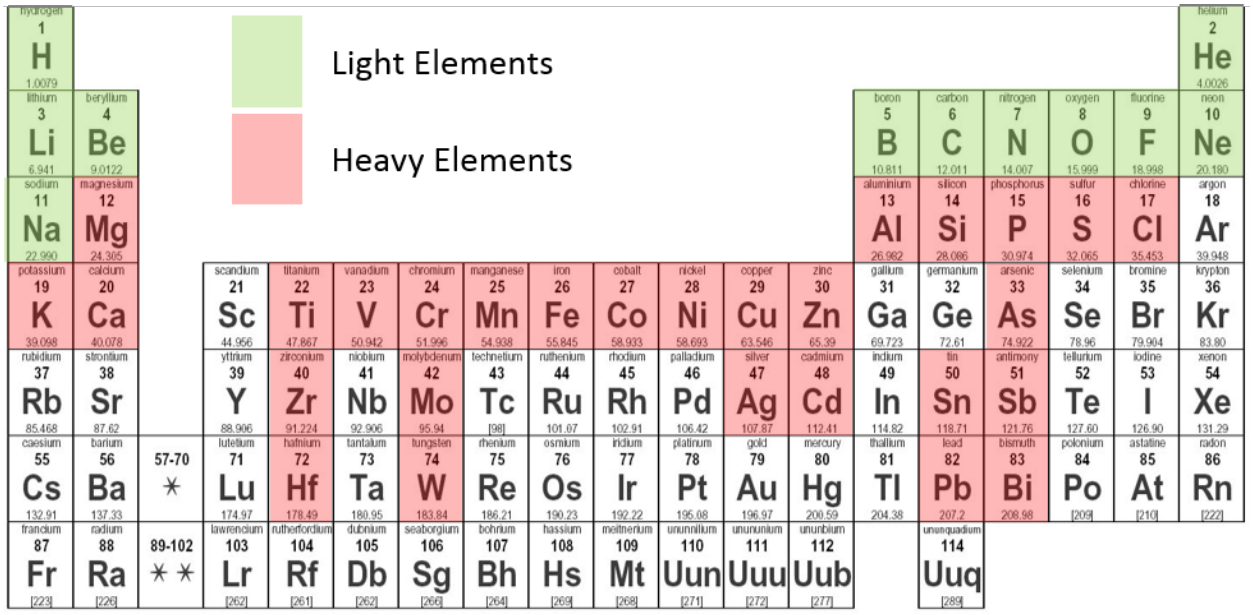

Figure 20: Periodic table showing elements measurable by the Innov-X® X-Ray Fluorescence Spectrometer.

The XRF spectrometer measures elemental abundances by subjecting the sample to X-ray photons. The high energy of the photons displaces inner orbital electrons in the respective elements. The vacancies in the lower orbitals cause outer orbital electrons to "fall" into lower orbits to satisfy the disturbed electron configuration. The substitution into lower orbitals causes a release of a secondary X-ray photon, which has an energy associated with a specific element. These relative and element specific energy emissions can then be used to determine bulk elemental composition.

3.2 MEDICAL CT SCANNING

Core scale CT scanning was done with a Toshiba® Aquilion TSX-101A/R medical scanner (medical CT) as shown in Figure 21. The medical CT scanner generates images with a resolution in the millimeter range, with scans having voxel resolutions of 0.43 x 0.43 mm in the XY plane and 0.50 mm along the core axis. The scans were conducted at a voltage of 135 kV and at 200 mA. Subsequent processing and combining of stacks was performed to create three-dimensional (3D) volumetric representations of the cores and a two-dimensional (2D) cross-section through the middle of the core samples using ImageJ (Rasband, 2018). The variation in grayscale values observed in the images indicates changes in the CT number obtained from the scans, which is directly proportional to changes in the attenuation and density of the scanned rock; i.e. darker regions are less dense. As can be seen in Figures 22–38, filled fractures, open fractures, and changes in bedding structure can be resolved via careful examination of the CT images. While the medical CT scanner was not used for detailed characterization in this study, it allowed for non-destructive bulk characterization of the core, and thus complimented the MSCL data on the resultant logs.

Figure 21: Medical CT at the NETL used for core analysis.

3.3 DATA COMPILATION

Strater® by Golden Software® was used to compile the MSCL and medical CT data into a series of geophysical logs. The data used to generate these logs can be accessed from NETL's EDX online system using the following link: https://edx.netl.doe.gov/dataset/armstrong-well.

4. RESULTS

Processed 2D slices of the medical CT scans through the cores are shown first, followed by the XRF and magnetic susceptibility measurements of the core from the MSCL.

4.1 MEDICAL CT SCANS

The majority of the core from the Armstrong #1 well was scanned with a Toshiba Aquilion TSX-101A/R medical CT scanner at a sub-millimeter core-scale resolution (430 μm by 430 μm by 500 μm). Five sub-sections were scanned at different resolutions in the X-Y plane ranging from 311 μm to 463 μm listed in Table 4 and a slice depth of 500 μm; these have been scaled in the following images to be the same resolution as the other scans.

Table 4: Core sections with different medical CT image resolution

Core Depth	X-Y Plane Resolution
7,545 to 7,548 ft	445 μm by 445 μm
7,548 to 7,551 ft	311 μm by 311 μm
7,556.8 to 7,559.75 ft	353 μm by 353 μm
7,565.75 to 7,568 ft	463 μm by 463 μm
7,605.5 to 7,606 ft	316 μm by 316 μm

Core was scanned in 3 ft or smaller sections obtained from each core box. In highly-fractured regions, the true length of these sections were frequently excess of 3 ft and detailed information in log books and photographs of cores were used to merge multiple scans of cores when this occurred. In the following images, the overall depth for each scanned sub-section of core is listed and many interesting features are apparent, including pyrite nodules, defined fracture planes and fine-scale layering.

4.2 ARMSTRONG #1

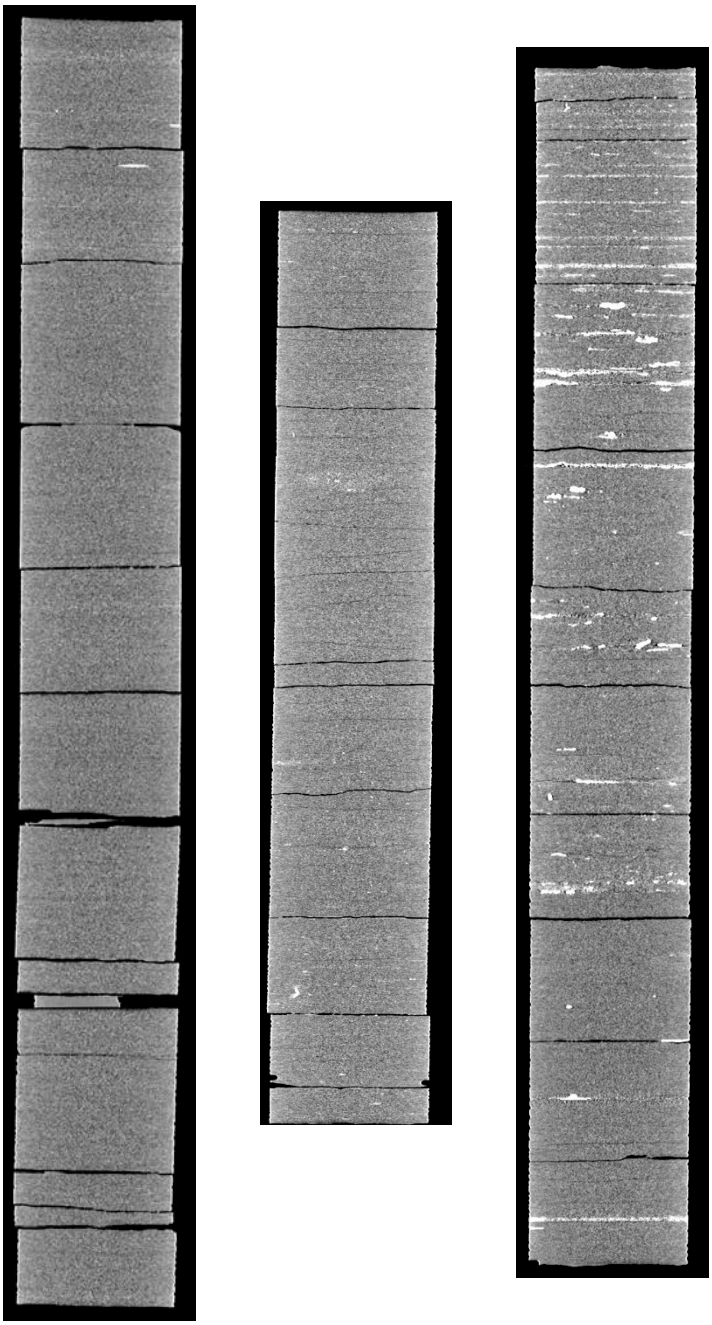

7,545–7,548 ft **7,548–7,551 ft** **7,551–7,553.8 ft**

Figure 22: 2D isolated planes through the vertical center of the medical CT scans of the Armstrong #1 core from 7,545 to 7,553.8 ft.

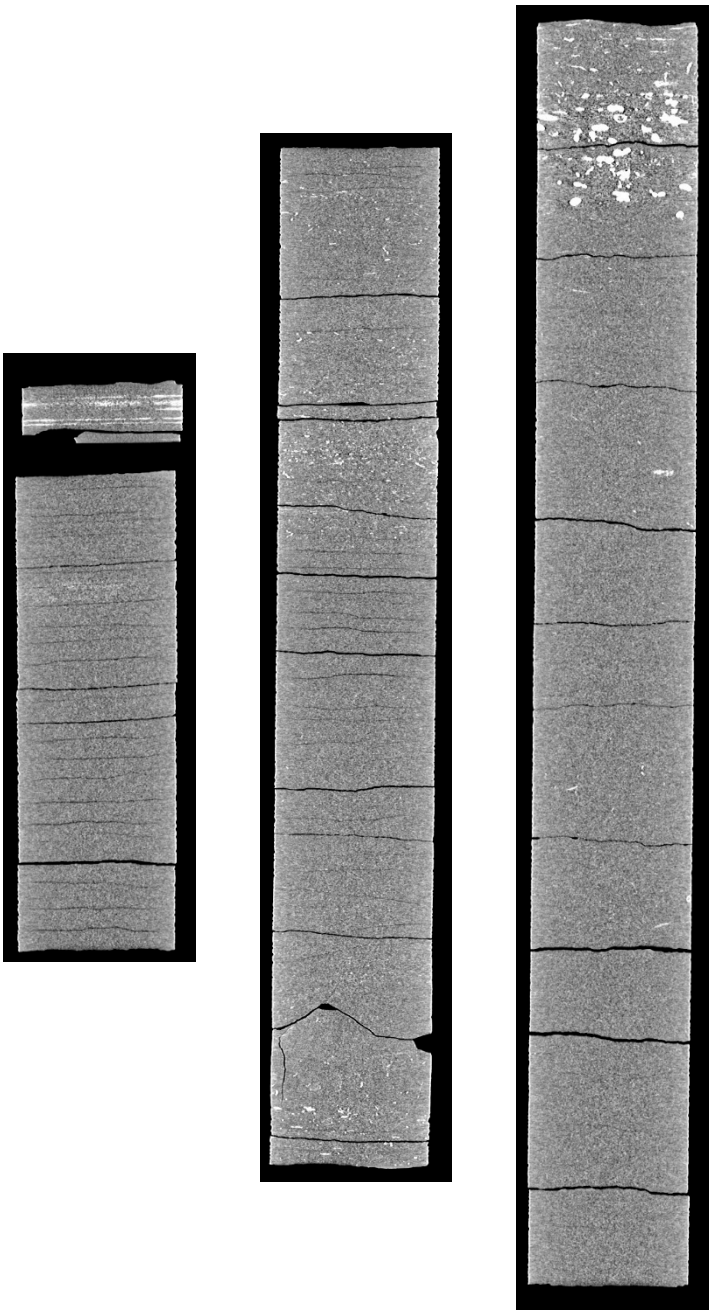

7,553.85–7,556.8 ft **7,556.8–7,559.75 ft** **7,559.75–7,562.75 ft**

Figure 23: 2D isolated planes through the vertical center of the medical CT scans of the Armstrong #1 core from 7,553.85 to 7,562.75 ft.

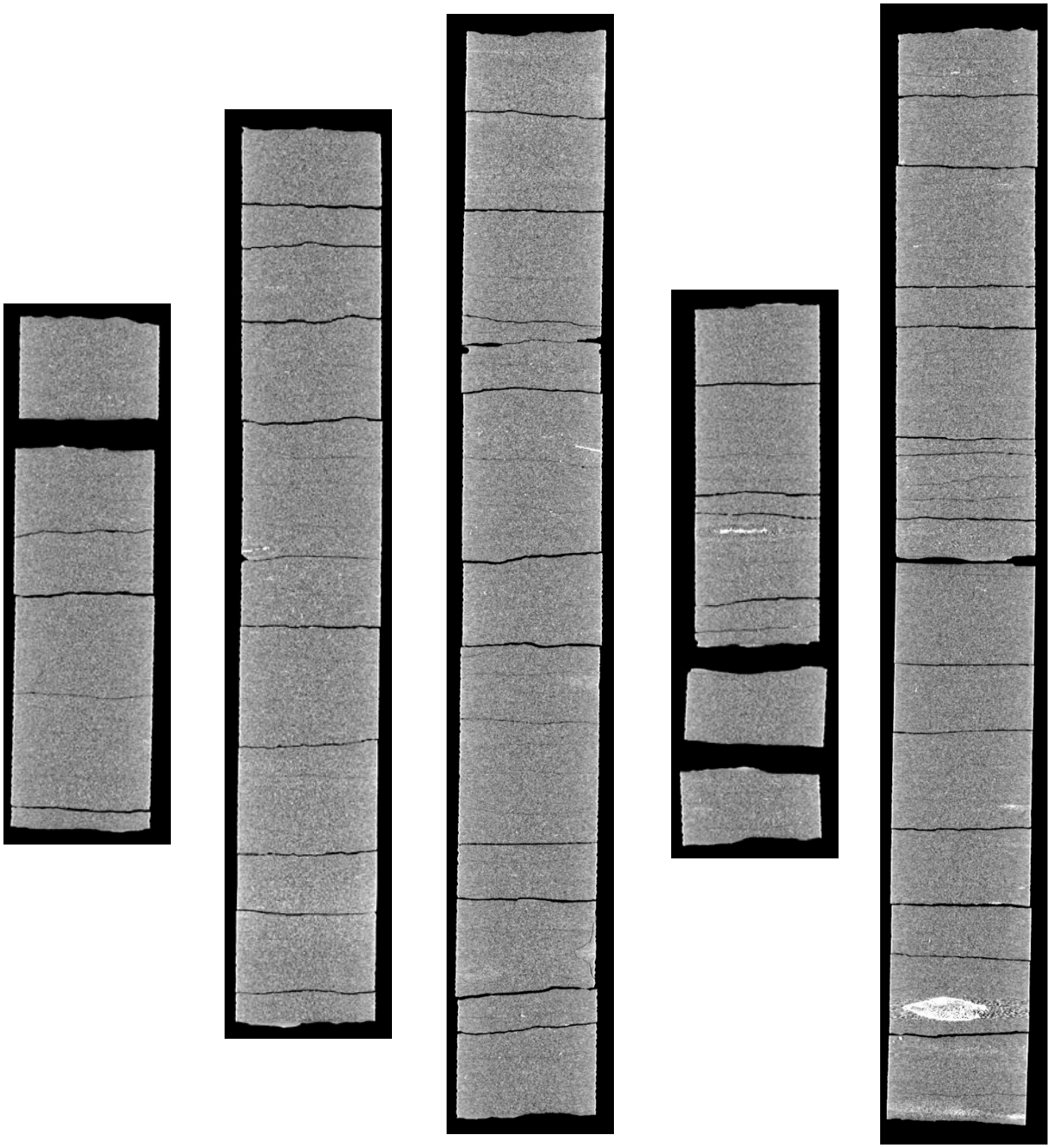

7,562.75–7,565.75 ft **7,565.75–7,568 ft** **7,568–7,571 ft** **7,571–7,574 ft** **7,574–7,577 ft**

Figure 24: 2D isolated planes through the vertical center of the medical CT scans of the Armstrong #1 core from 7,562.75 to 7,577 ft.

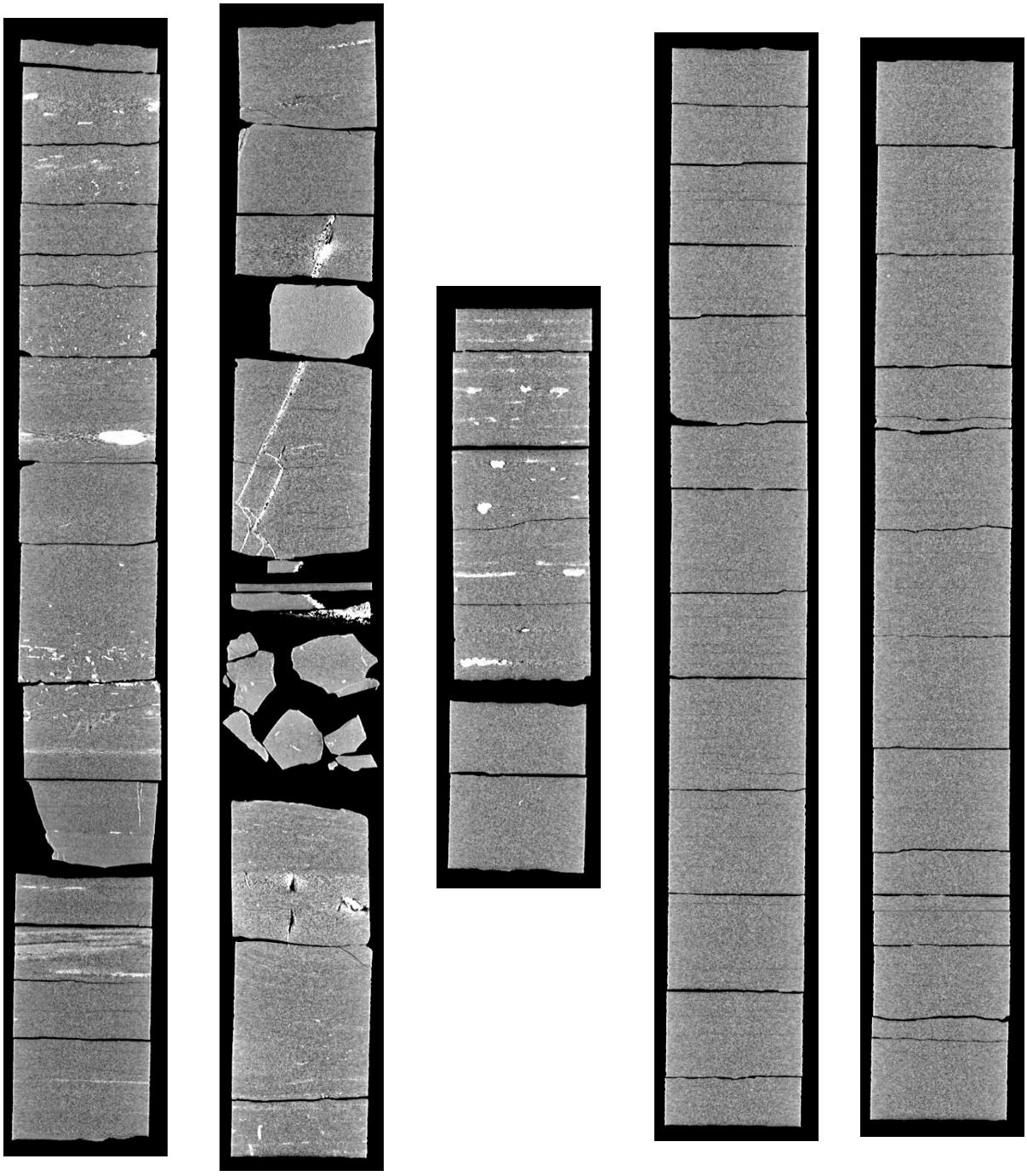

7,577–7,580 ft **7,580–7,583 ft** **7,583–7,586 ft** **7,586–7,589 ft** **7,589–7,592 ft**

Figure 25: 2D isolated planes through the vertical center of the medical CT scans of the Armstrong #1 core from 7,577 to 7,592 ft.

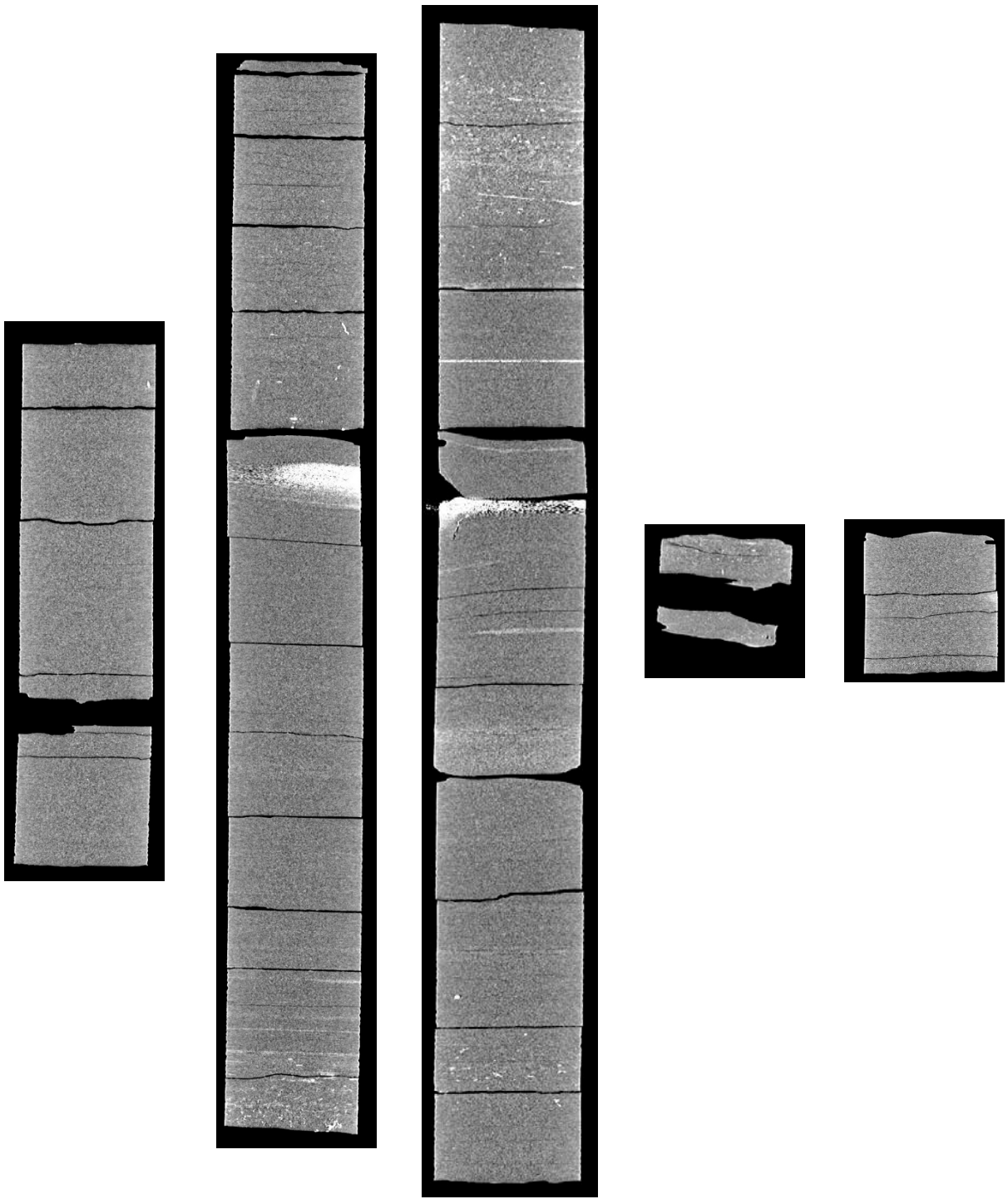

7,592–7,595 ft **7,595–7,598 ft** **7,598–7,601 ft** **7,604–7,605.5 ft** **7,605.5–7,606 ft**

Figure 26: 2D isolated planes through the vertical center of the medical CT scans of the Armstrong #1 core from 7,592 to 7,606 ft.

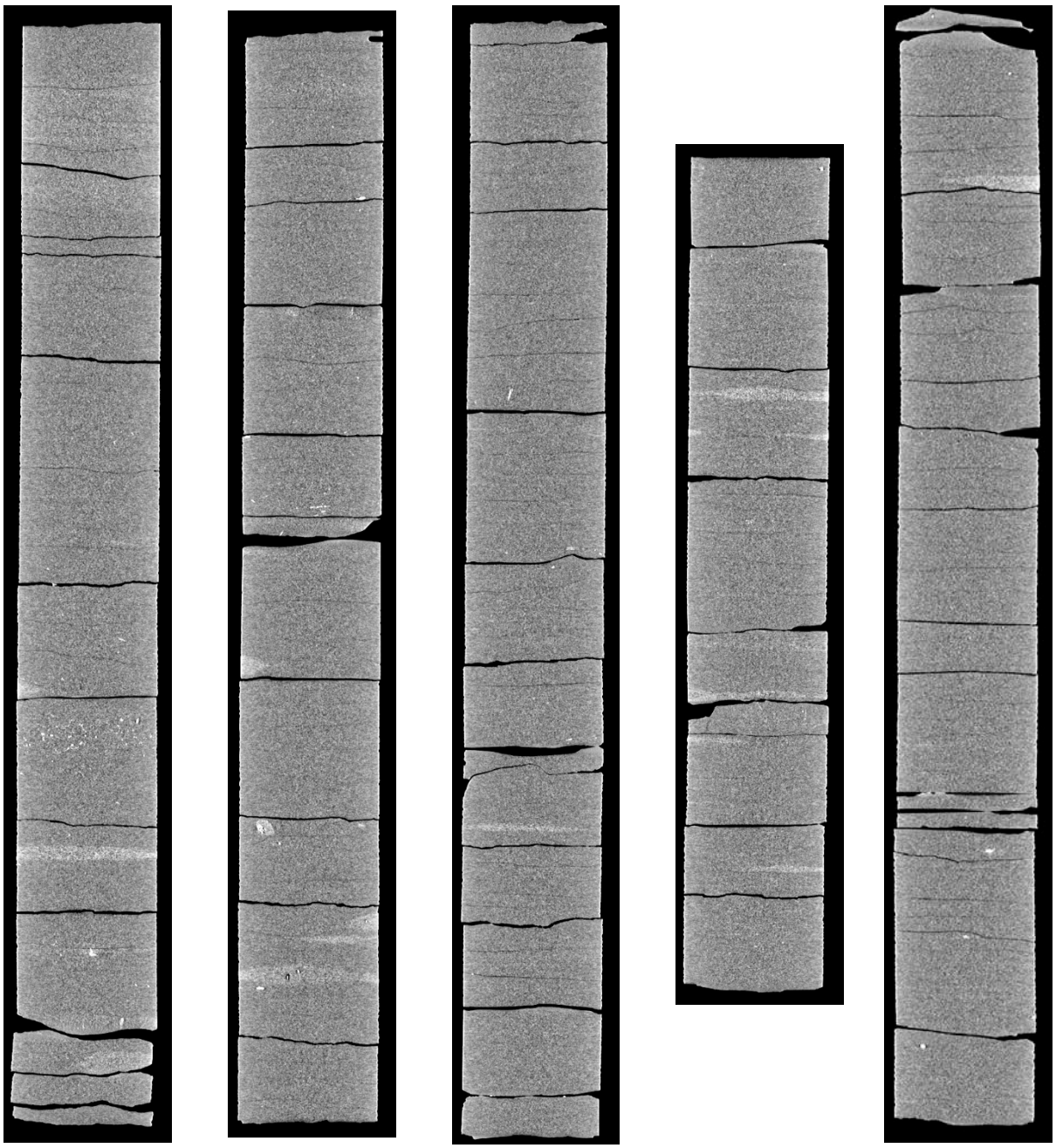

7,606–7,609 ft **7,609–7,612 ft** **7,612–7,615 ft** **7,615–7,618 ft** **7,618–7,621 ft**

Figure 27: 2D isolated planes through the vertical center of the medical CT scans of the Armstrong #1 core from 7,606 to 7,621 ft.

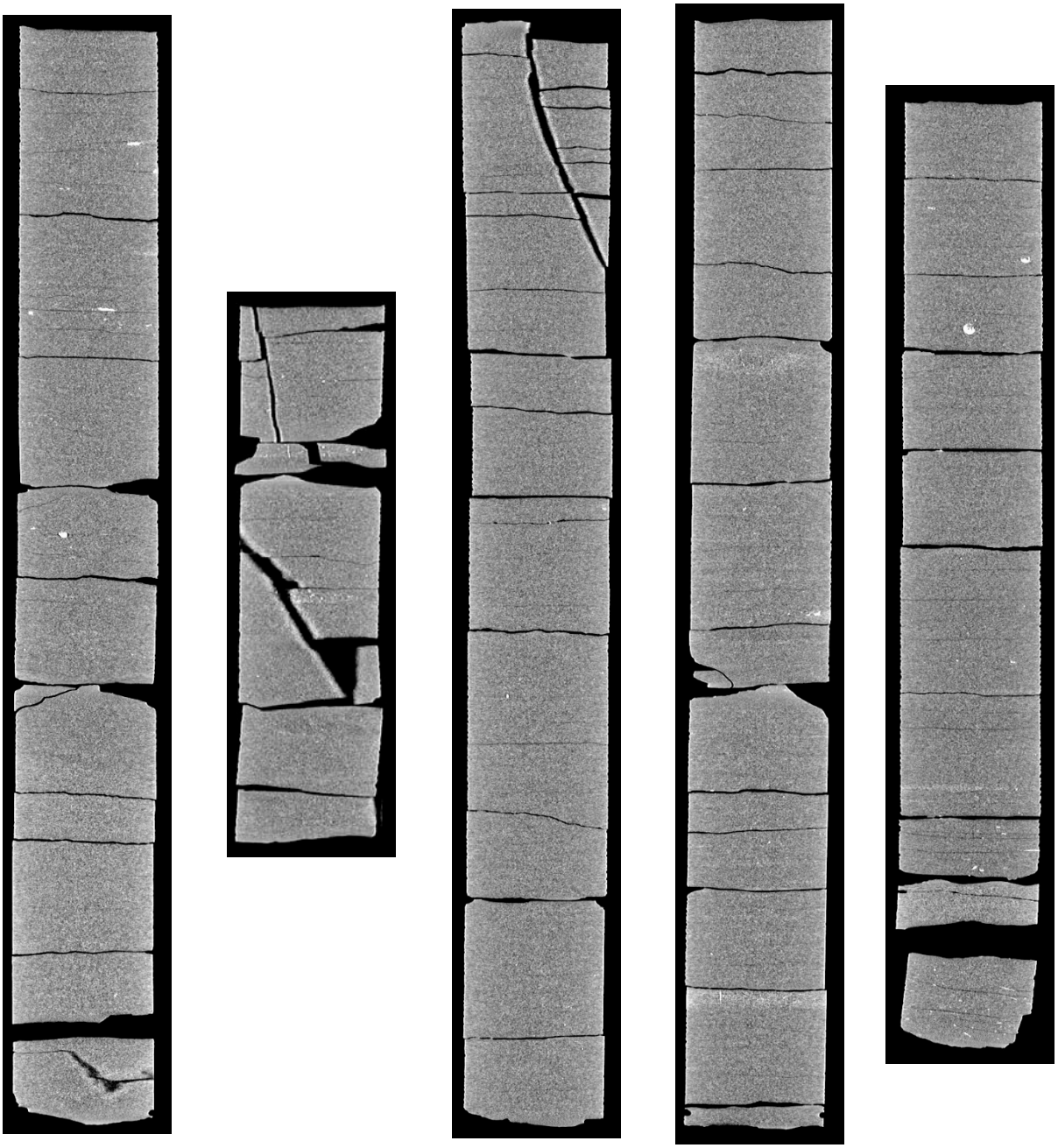

7,621–7,624 ft **7,624–7,627 ft** **7,627–7,630 ft** **7,630–7,633 ft** **7,633–7,636 ft**

Figure 28: 2D isolated planes through the vertical center of the medical CT scans of the Armstrong #1 core from 7,621 to 7,636 ft.

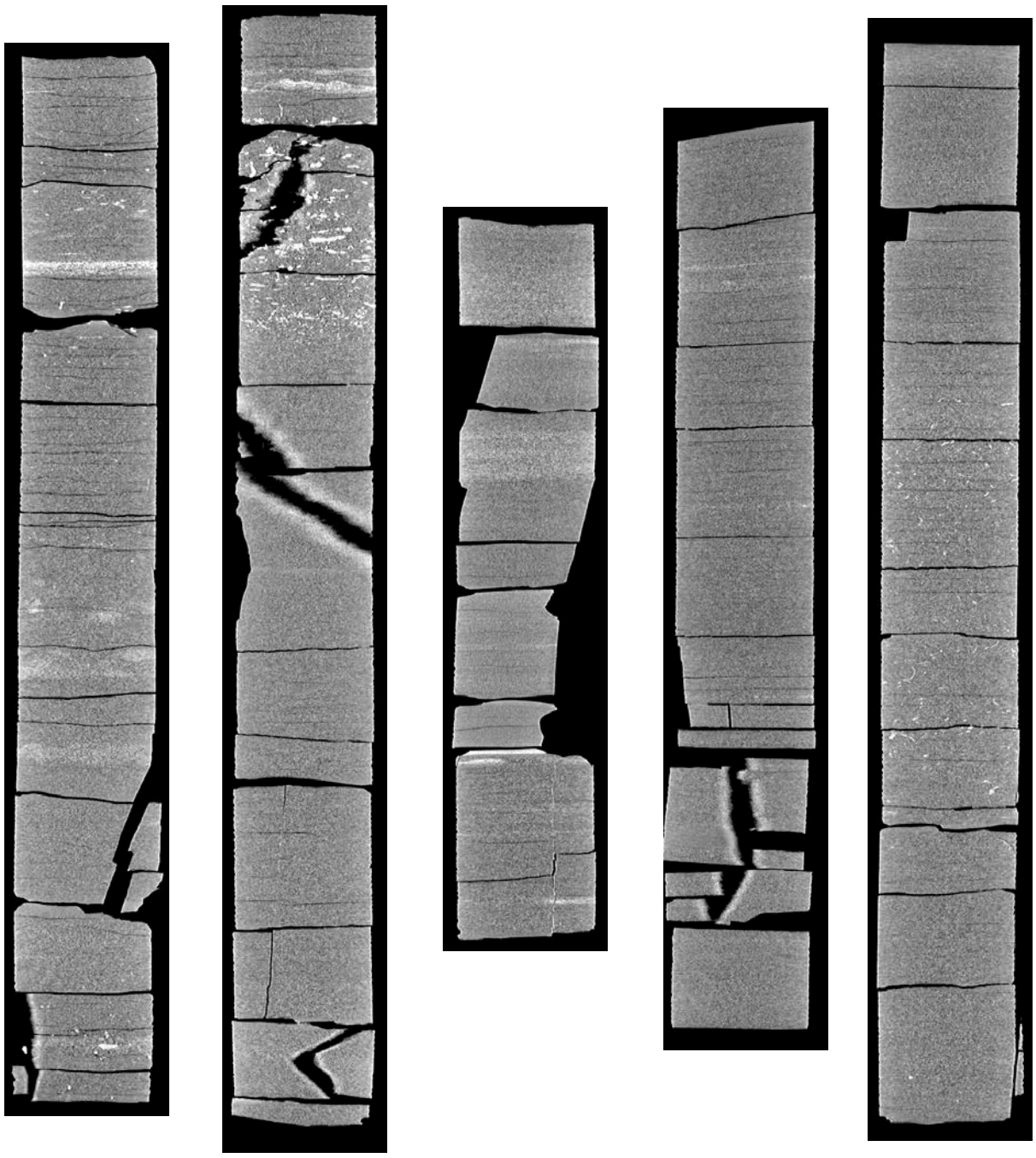

7,636–7,639 ft **7,639–7,642 ft** **7,642–7,645 ft** **7,645–7,648 ft** **7,648–7,651 ft**

Figure 29: 2D isolated planes through the vertical center of the medical CT scans of the Armstrong #1 core from 7,636 to 7,651 ft.

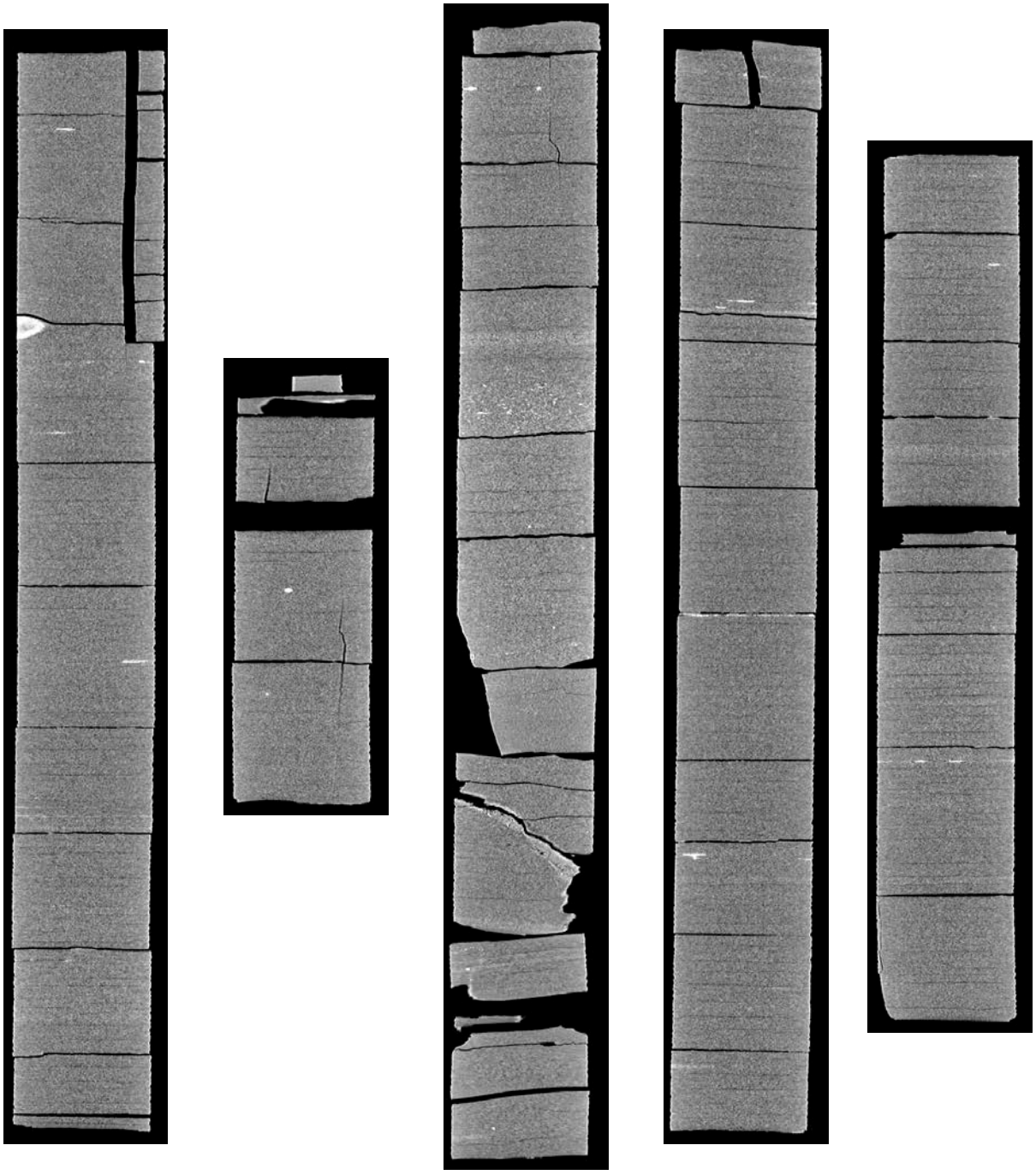

7,651–7,654 ft **7,654–7,657 ft** **7,657–7,660 ft** **7,660–7,663 ft** **7,663–7,666 ft**

Figure 30: 2D isolated planes through the vertical center of the medical CT scans of the Armstrong #1 core from 7,651 to 7,666 ft.

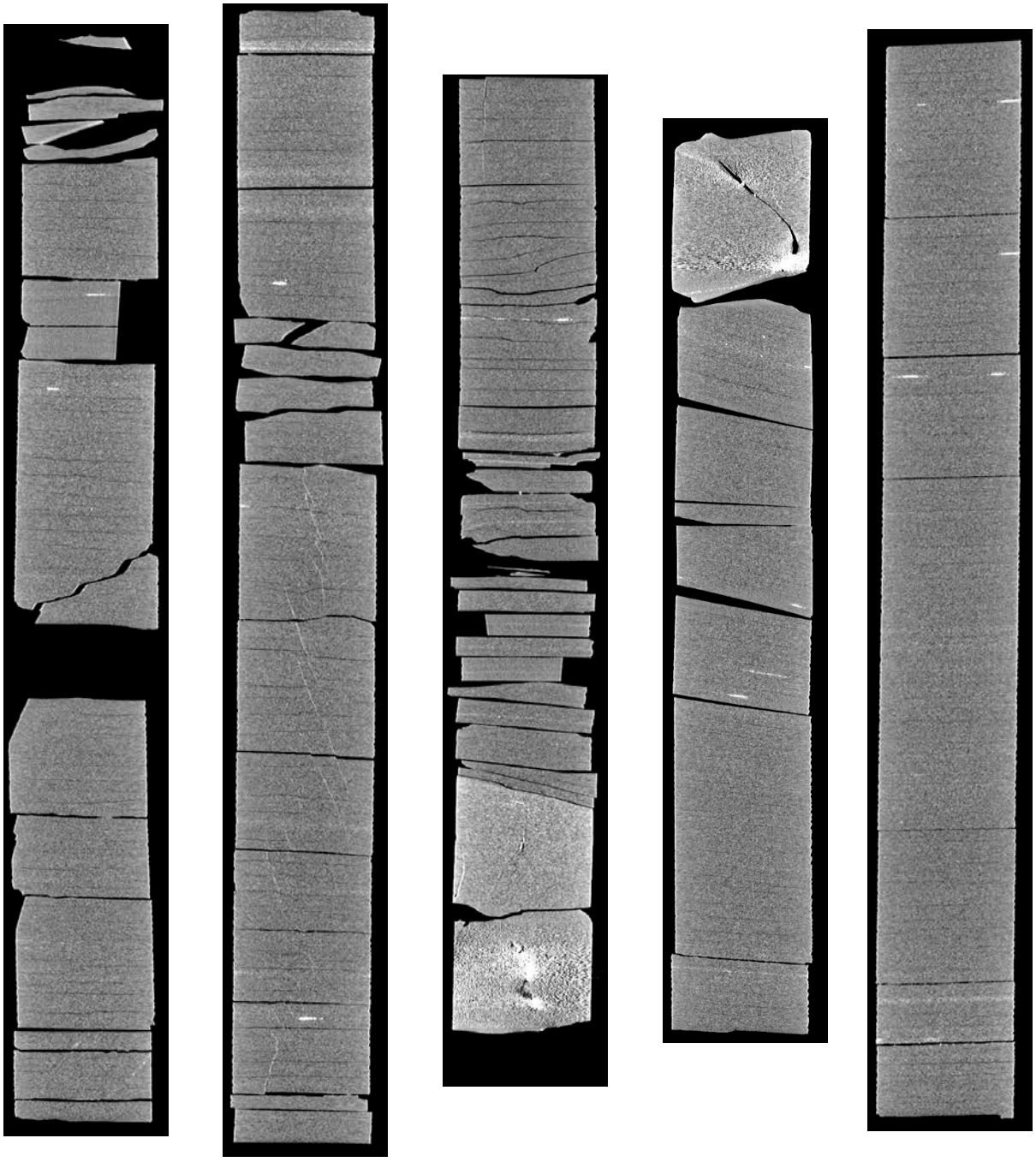

7,666.3–7,669 ft **7,669–7,672 ft** **7,672–7,675 ft** **7,675–7,678 ft** **7,678–7,681 ft**

Figure 31: 2D isolated planes through the vertical center of the medical CT scans of the Armstrong #1 core from 7,666.3 to 7,681 ft.

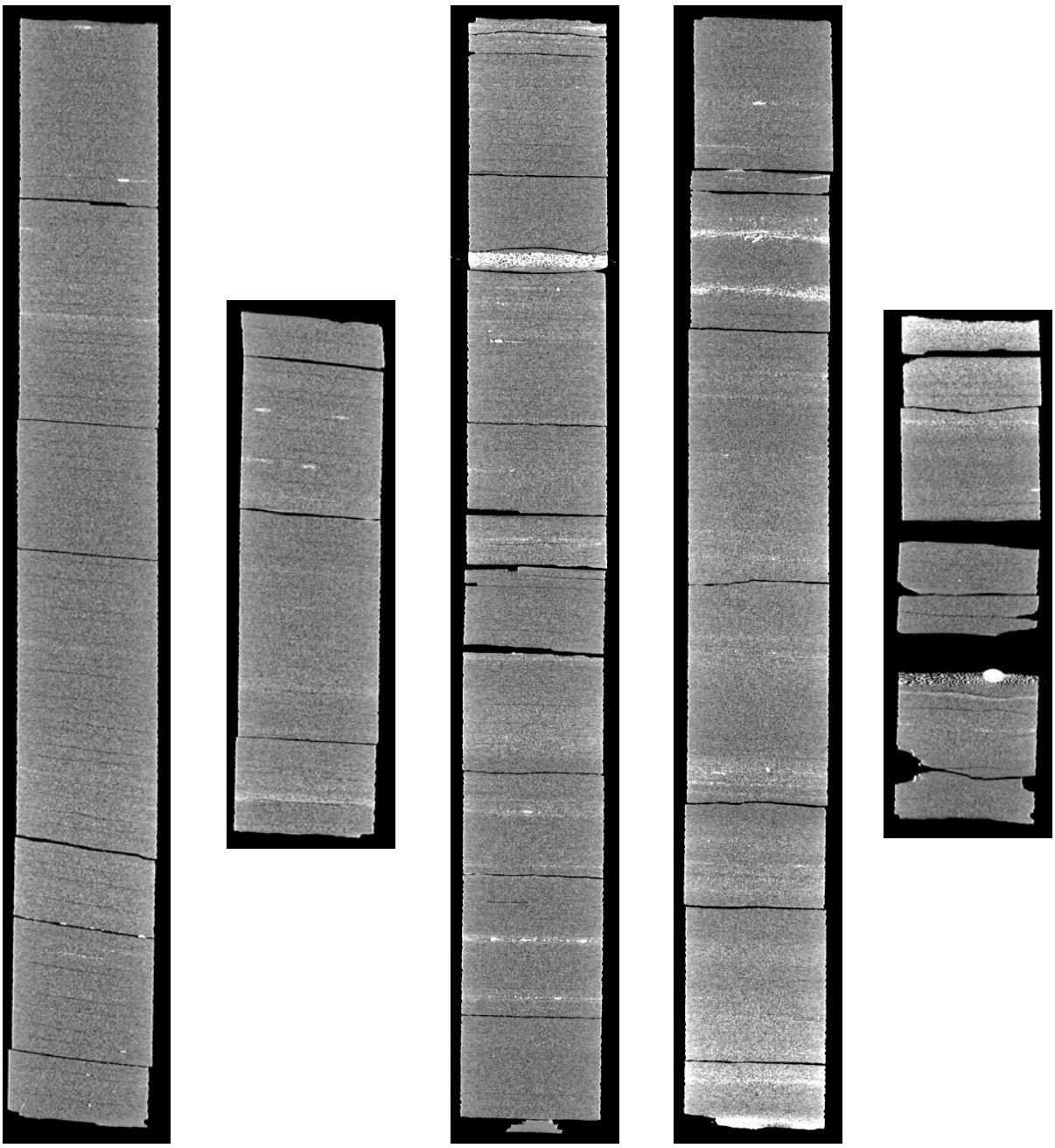

7,681–7,684 ft **7,684–7,687 ft** **7,687–7,690 ft** **7,690–7,693 ft** **7,693–7,696 ft**

Figure 32: 2D isolated planes through the vertical center of the medical CT scans of the Armstrong #1 core from 7,681 to 7,696 ft.

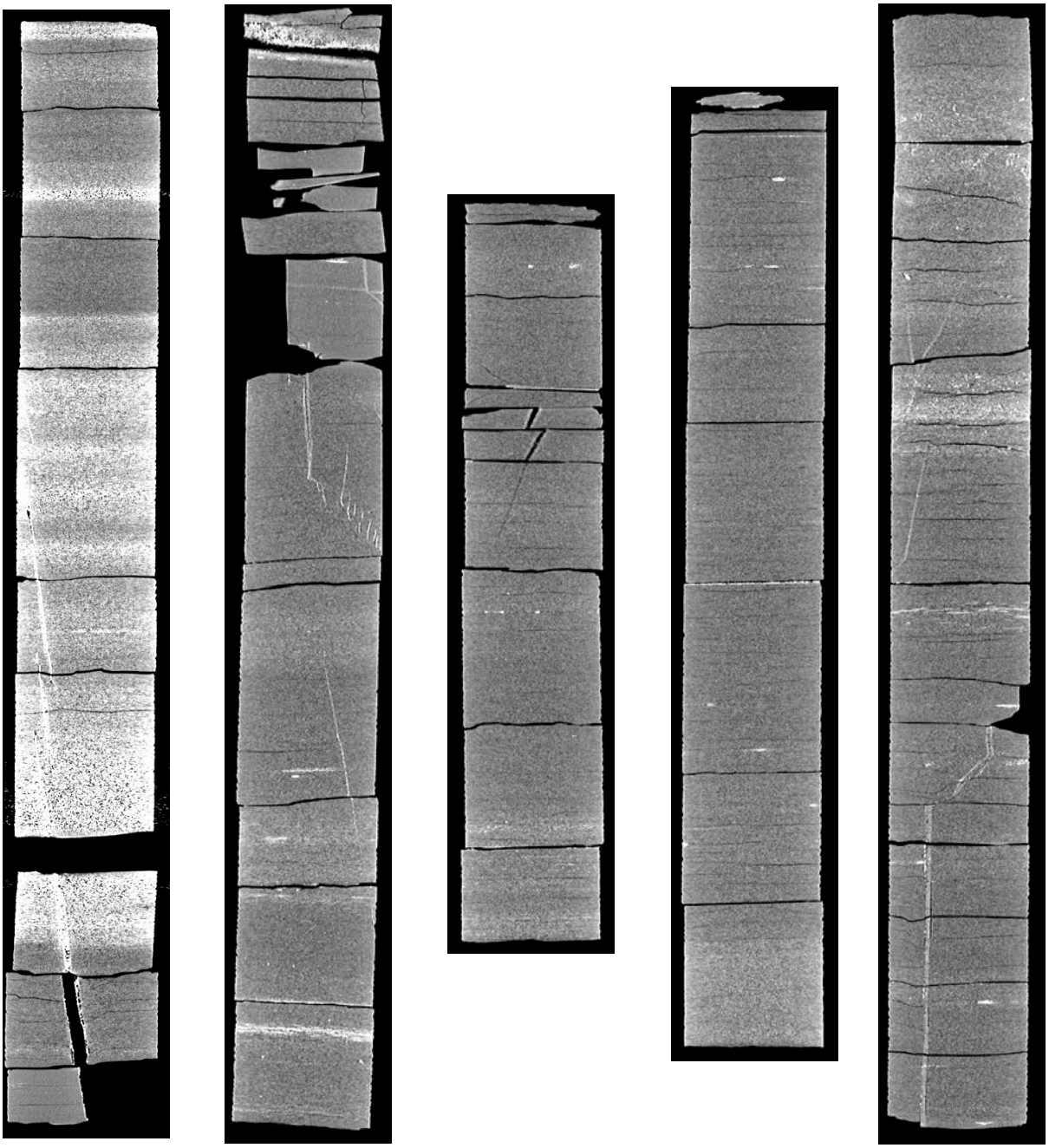

7,696–7,699 ft **7,699–7,702 ft** **7,702–7,705 ft** **7,705–7,708 ft** **7,708–7,711 ft**

Figure 33: 2D isolated planes through the vertical center of the medical CT scans of the Armstrong #1 core from 7,696 to 7,711 ft.

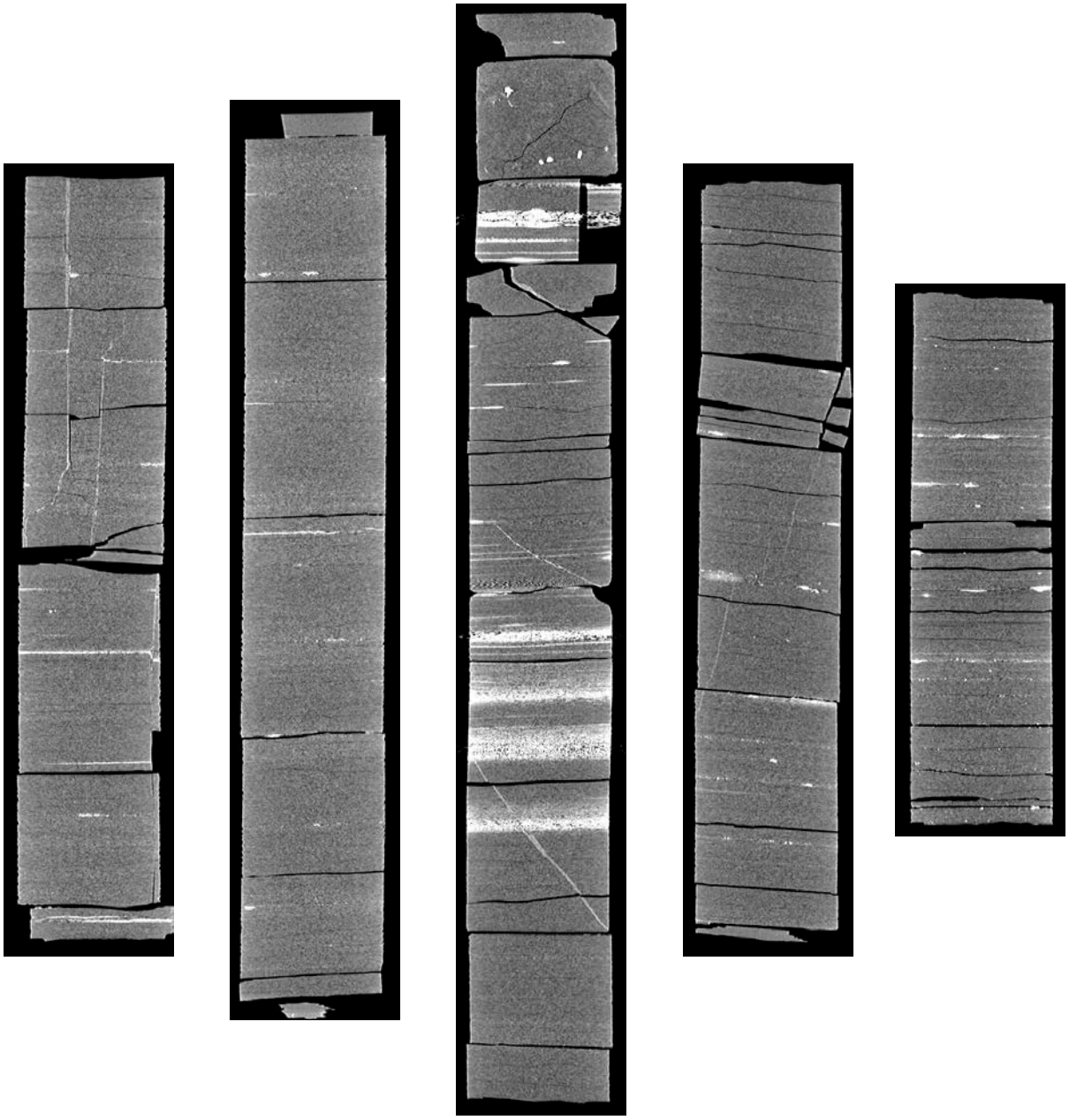

7,711–7,714 ft **7,714–7,717 ft** **7,717–7,720 ft** **7,720–7,723 ft** **7,723–7,724.6 ft**

Figure 34: 2D isolated planes through the vertical center of the medical CT scans of the Armstrong #1 core from 7,711 to 7,724.6 ft.

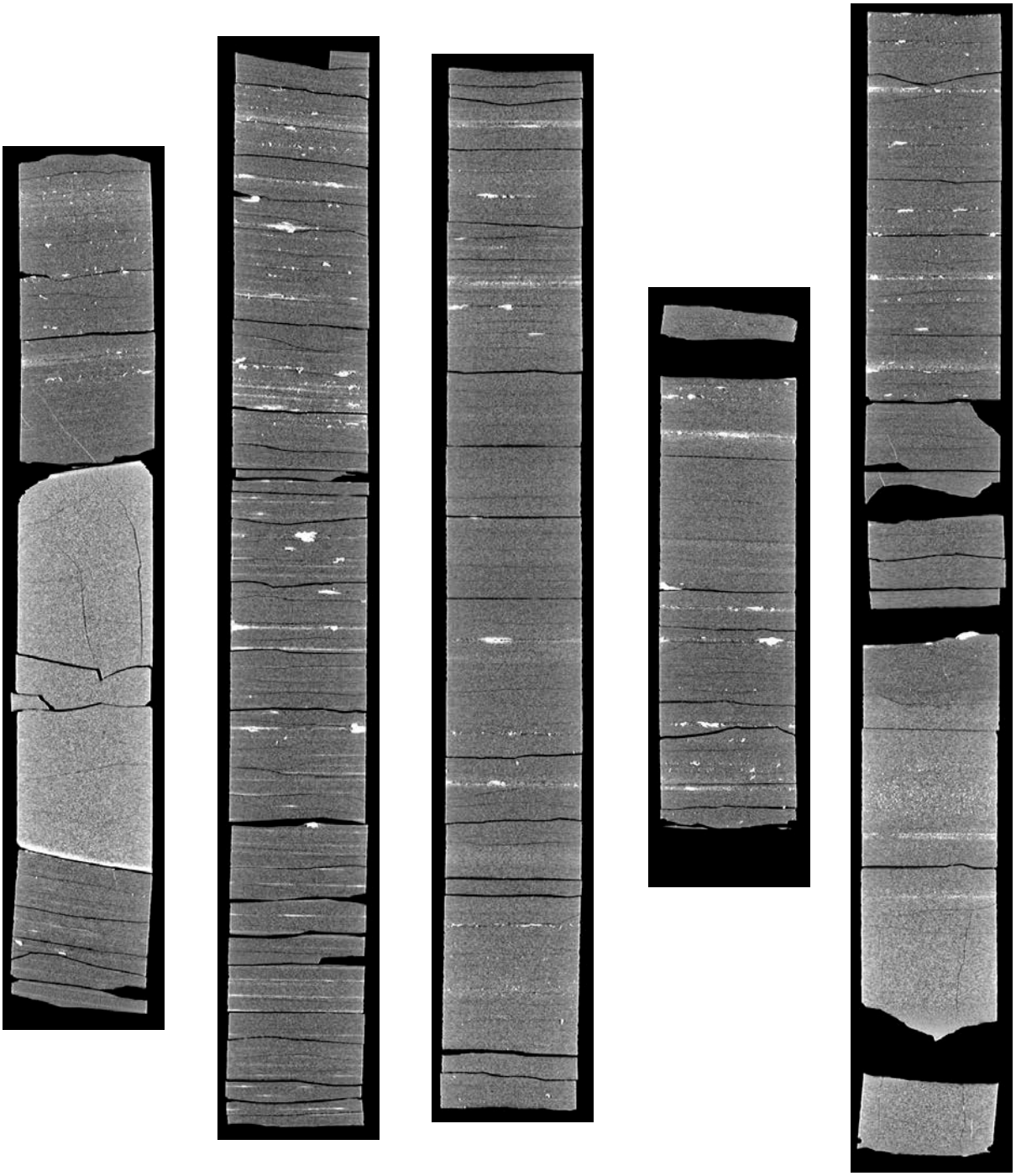

7,724.6–7,727 ft **7,727–7,730 ft** **7,730–7,732.9 ft** **7,732.9–7,736 ft** **7,736–7,739 ft**

Figure 35: 2D isolated planes through the vertical center of the medical CT scans of the Armstrong #1 core from 7,724.6 to 7,739 ft.

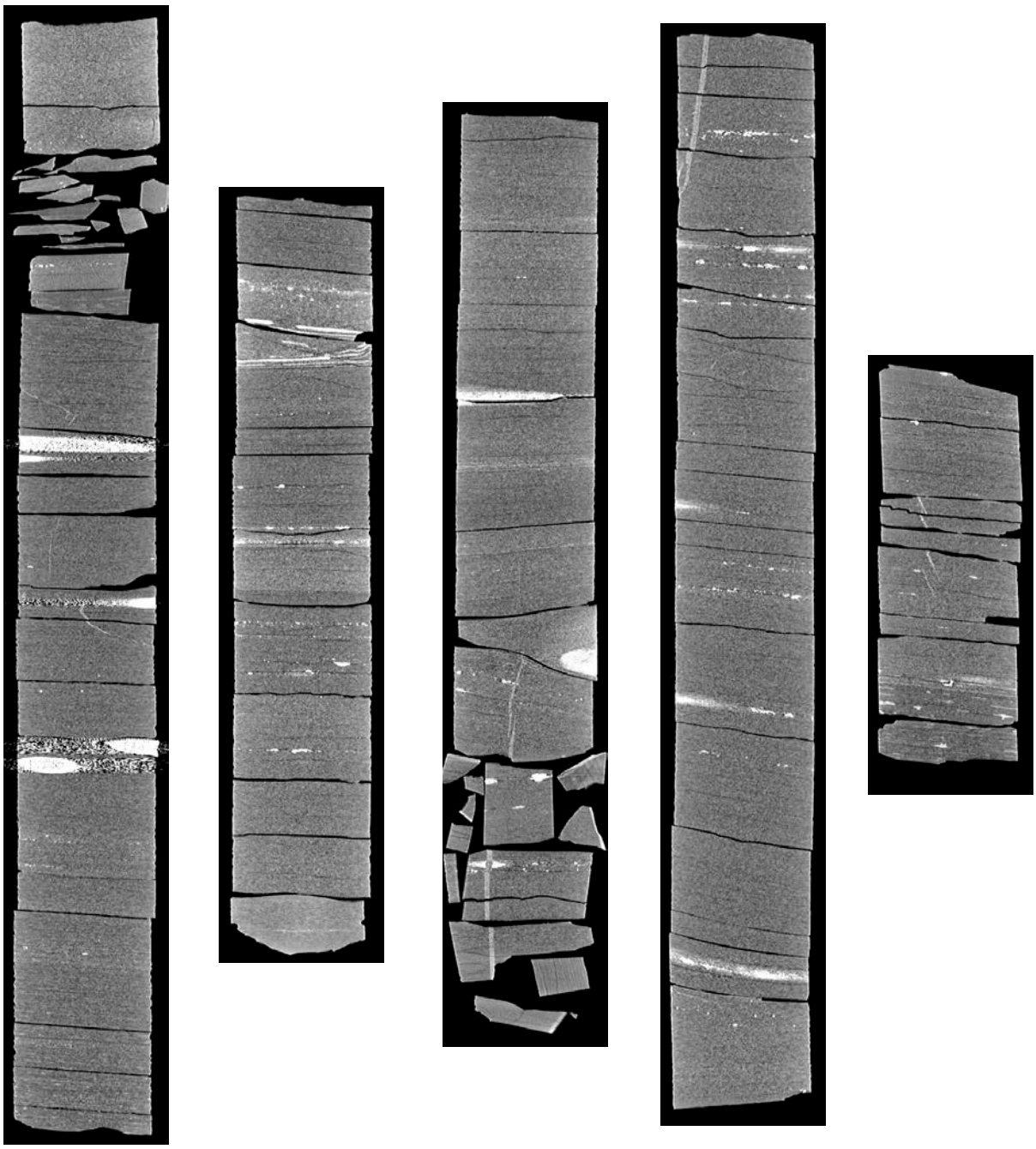

7,739–7,742 ft **7,742–7,745 ft** **7,745–7,748 ft** **7,748–7,751 ft** **7,751–7,754 ft**

Figure 36: 2D isolated planes through the vertical center of the medical CT scans of the Armstrong #1 core from 7,739 to 7,754 ft.

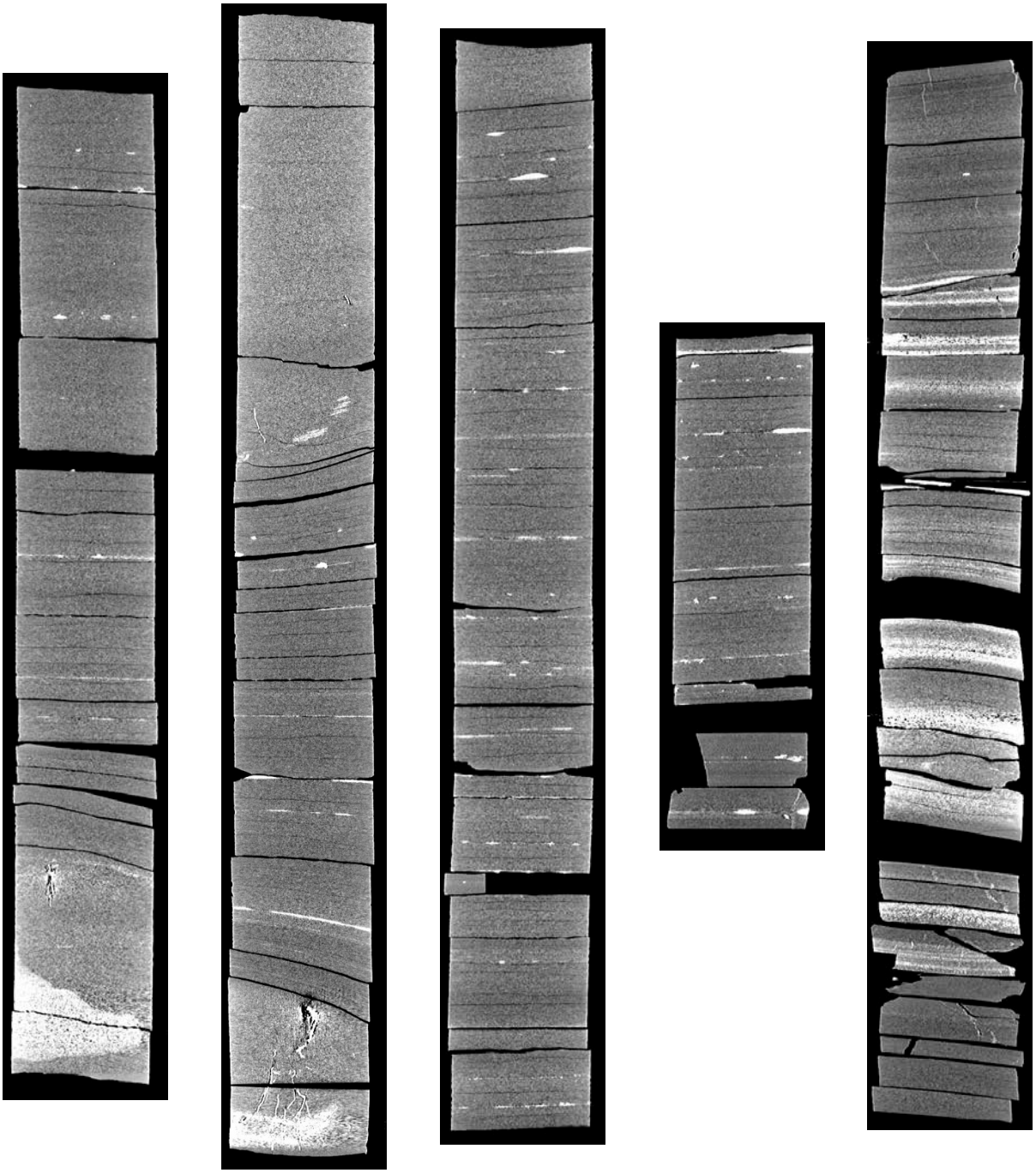

7,754–7,757 ft **7,757–7,760 ft** **7,760–7,763 ft** **7,763–7,766 ft** **7,766–7,769 ft**

Figure 37: 2D isolated planes through the vertical center of the medical CT scans of the Armstrong #1 core from 7,754 to 7,769 ft.

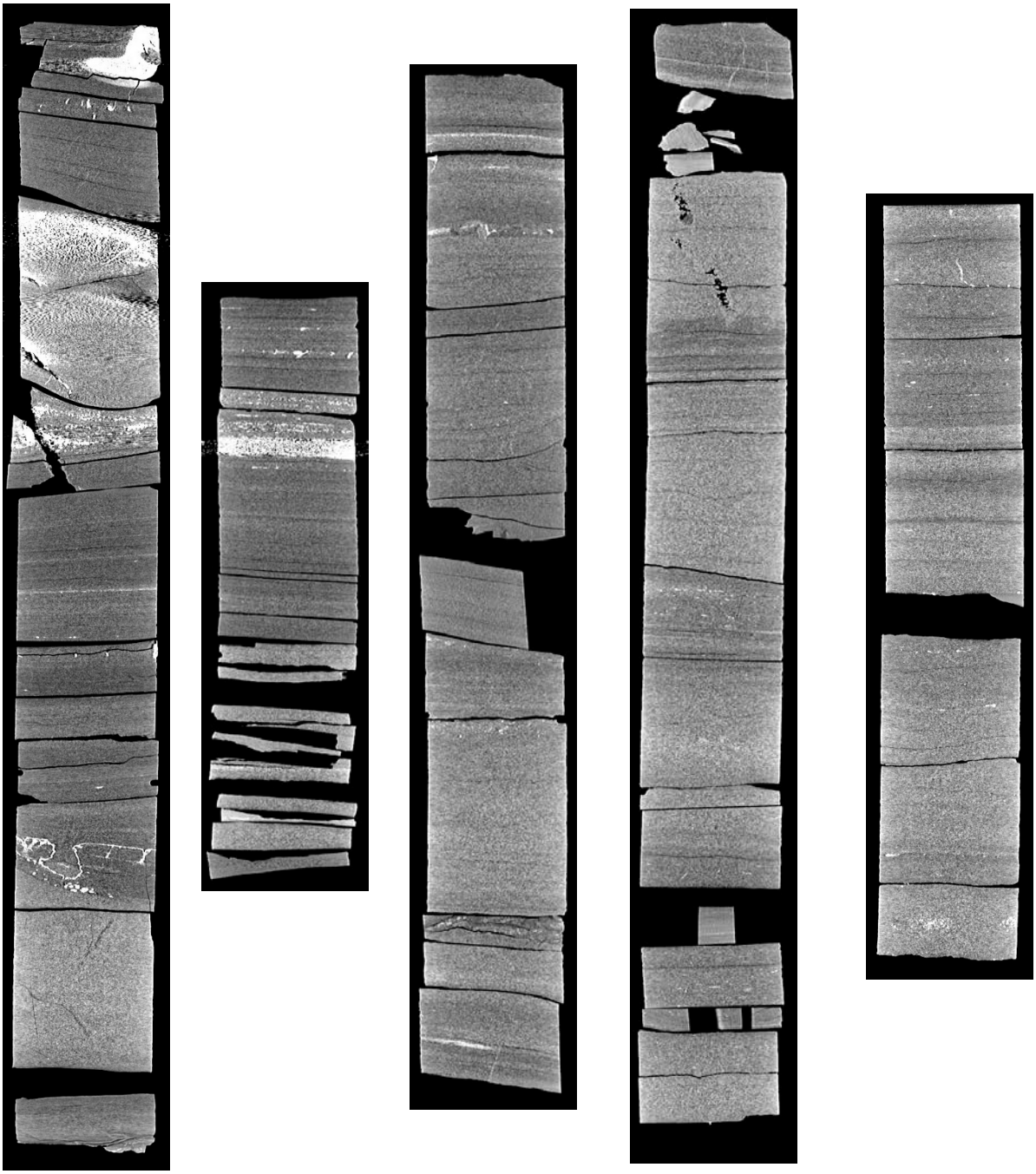

7,769–7,771.9 ft **7,771.9–7,775 ft** **7,775–7,778 ft** **7,778–7,781 ft** **7,781–7,783.4 ft**

Figure 38: 2D isolated planes through the vertical center of the medical CT scans of the Armstrong #1 core from 7,769 to 7,783.4 ft.

4.3 ADDITIONAL CT DATA

Additional CT data can be accessed from NETL's EDX online system using the following link: https://edx.netl.doe.gov/dataset/armstrong-well. The original CT data is available as 16-bit tif stacks suitable for reading with ImageJ (Rasband, 2018) or other image analysis software. In addition, videos showing the variation along the length of the cross-section images shown in the previous section are available for download and viewing. A single image from these videos is shown in Figure 39, where the distribution of high-density minerals in a cross section of the core around a depth of 7,637.5 ft is shown. The red line through the on the XZ-plane image of the core shows the location of the XY-plane displayed above. The videos on EDX show this XY variation along the entire length of the core.

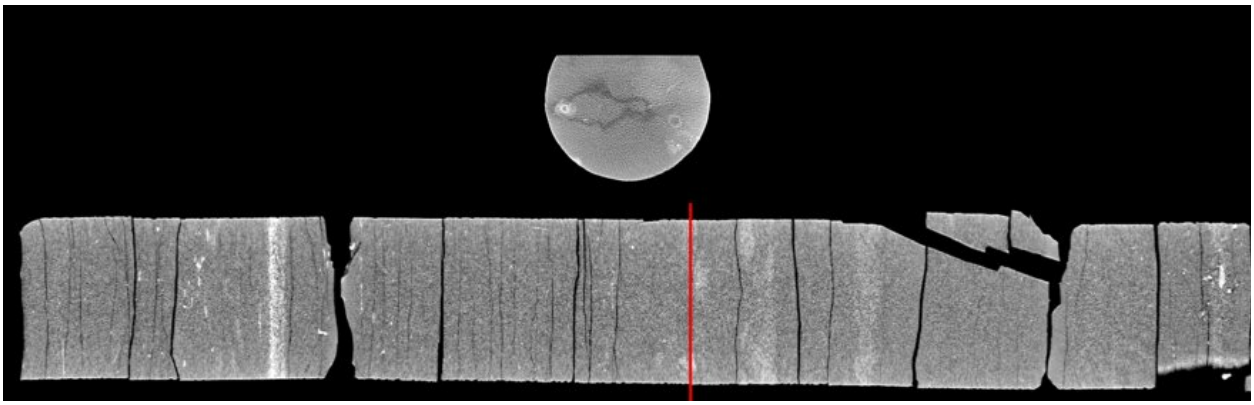

Figure 39: Single image from a video file available on EDX showing variation in the Armstrong #1 core from 7,636 to 7,639 ft. Image above shows the variation in composition within the matrix perpendicular to the core length. Note the bright (high density) nodules in the matrix and the cross-cutting fractured zone.

4.4 COMPILED CORE LOG

The compiled core logs were scaled to fit on single pages for rapid review of the combined data from the medical CT scans and MSCL readings. Two sets of logs are presented for the core; the first set with data from the CT scans and XRF, and the second set with calculated ratios from the XRF scans, P-wave data, and notable features. Features that can be derived from these combined analyses include determination of mineral locations, such as pyrite, from magnetic susceptibility and using the XRF to inform geochemical composition and mineral form.

Data from the MSCL that was obtained with P-wave velocity less than 330 m/s has been removed from these logs. This low P-wave velocity is less than the anticipated velocity through air, indicating a highly fractured zone and unreliable readings. The location of these fractured zones was confirmed through visual examination and with the medical CT scanned images.

The elemental results from the XRF were limited to Ca, Si and the remaining top nine elements (Fe, Ti, S, Al, V, K, Zn, Cd, and Mn). Of the remaining top nine elements, Fe was the most abundant with a maximum occurrence of 150,289 ppm at one location in the core, and Cd was the least abundant element with a maximum occurrence of 534 ppm at one location in the core.

All other elements measured, but not listed, were observed to have maximum occurrences of less than 6,700 ppm.

Trends in elemental ratios can provide insight into mineral composition, oxidation state, and depositional setting. Examples include: Ca/Si, which provides information on relative abundance of calcium carbonates versus silicates; Ca/Al, which gives approximate amounts of calcium carbonate versus clays and feldspars; Si/Al, which provides information on the abundance of illite and micas versus other clays, and Fe/S, which provides information on the abundance of pyrite versus Fe oxide minerals. Magnetic susceptibility can test for iron sulfides (reducing) or oxidized Fe and sulfate. Pyrite (reduced) should have low magnetic susceptibility, Fe oxide or hydroxide should have high magnetic susceptibility. Natural gamma is a proxy for organic carbon as well. These broad trends can quickly give information on large suites of core and direct more focused research. These logs are presented in Figures 40–43.

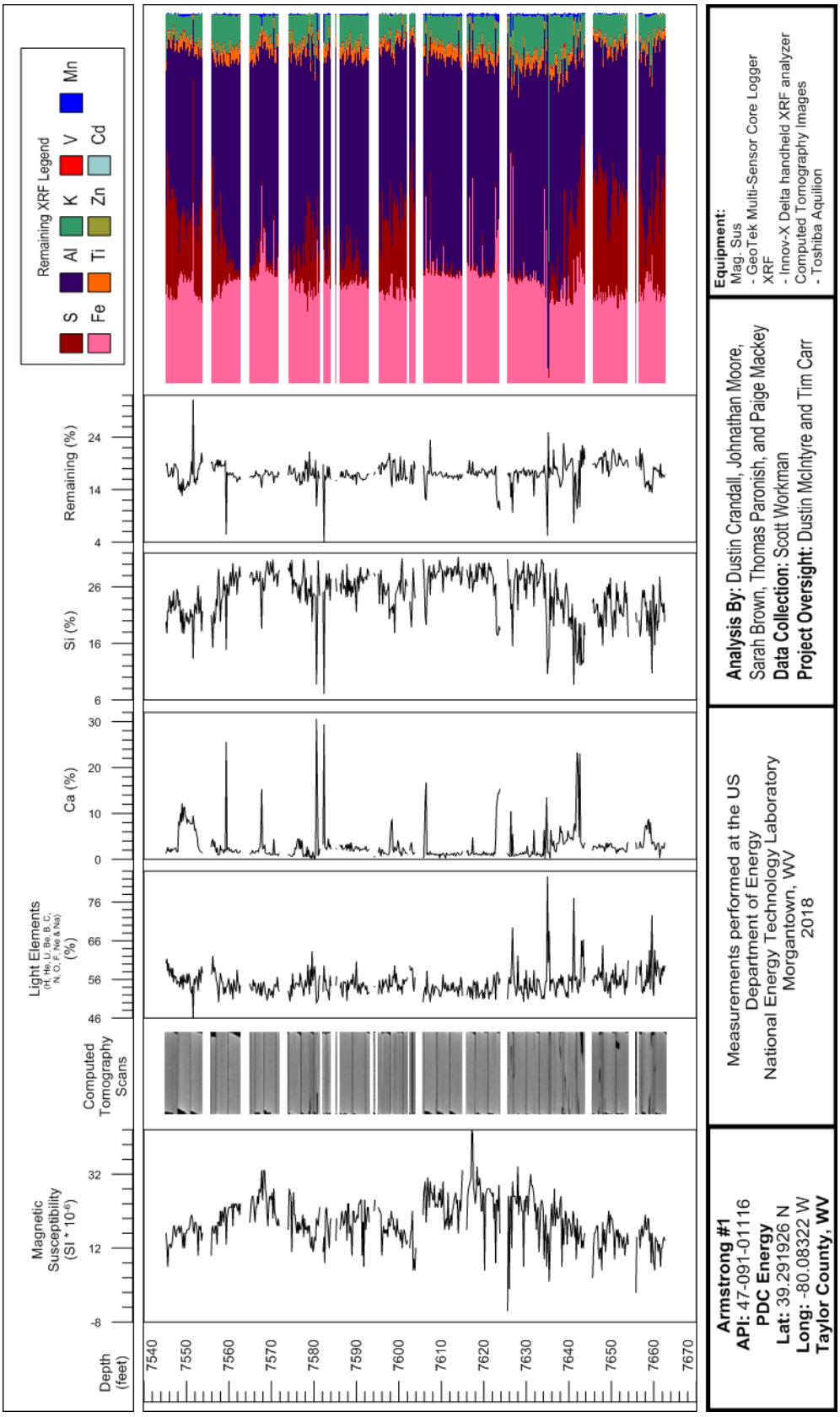

Figure 40: Compiled core log for Armstrong #1, from 7,545 to 7,662.5 ft.

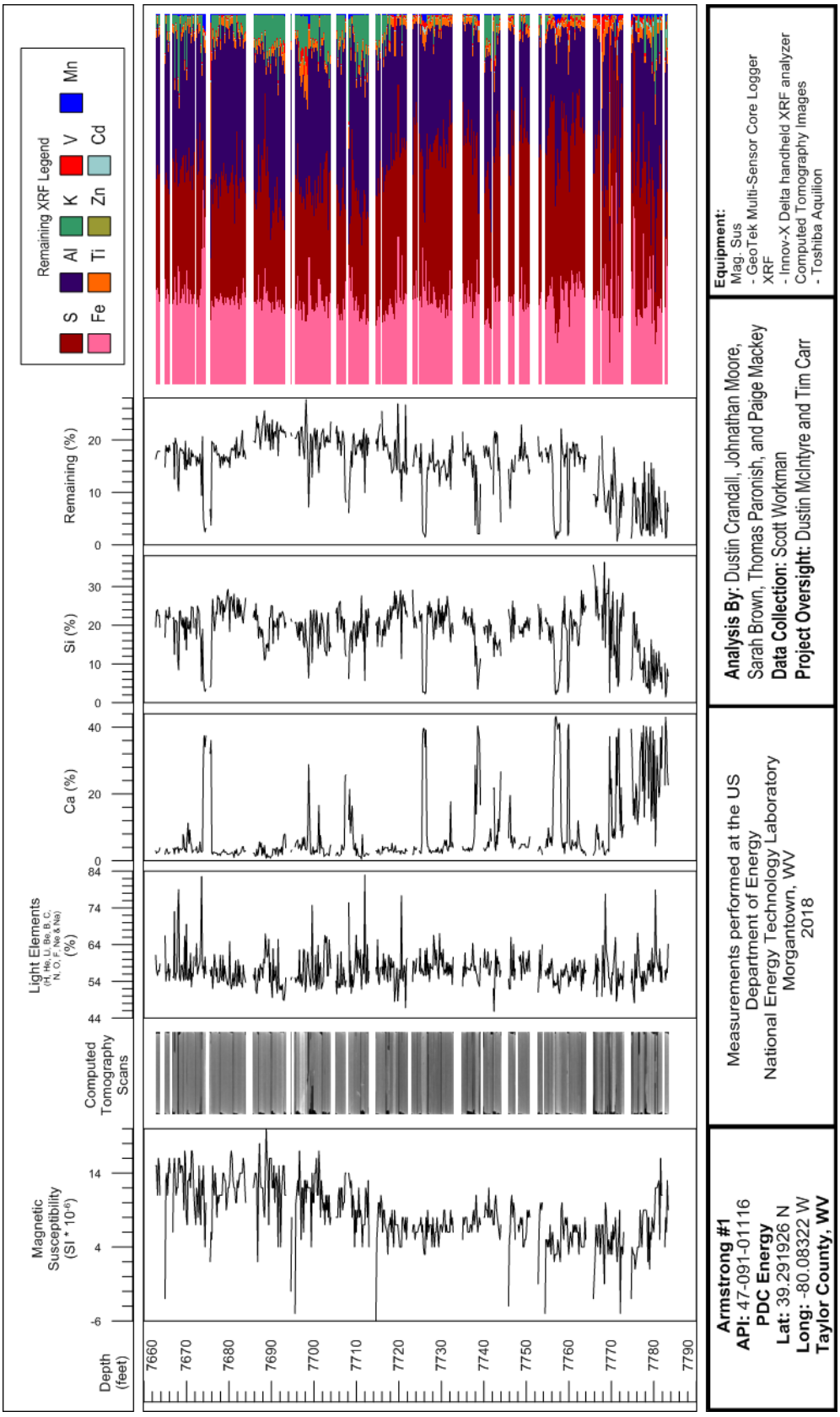

Figure 41: Compiled core log for Armstrong #1, from 7,662.5 to 7,783.4 ft.

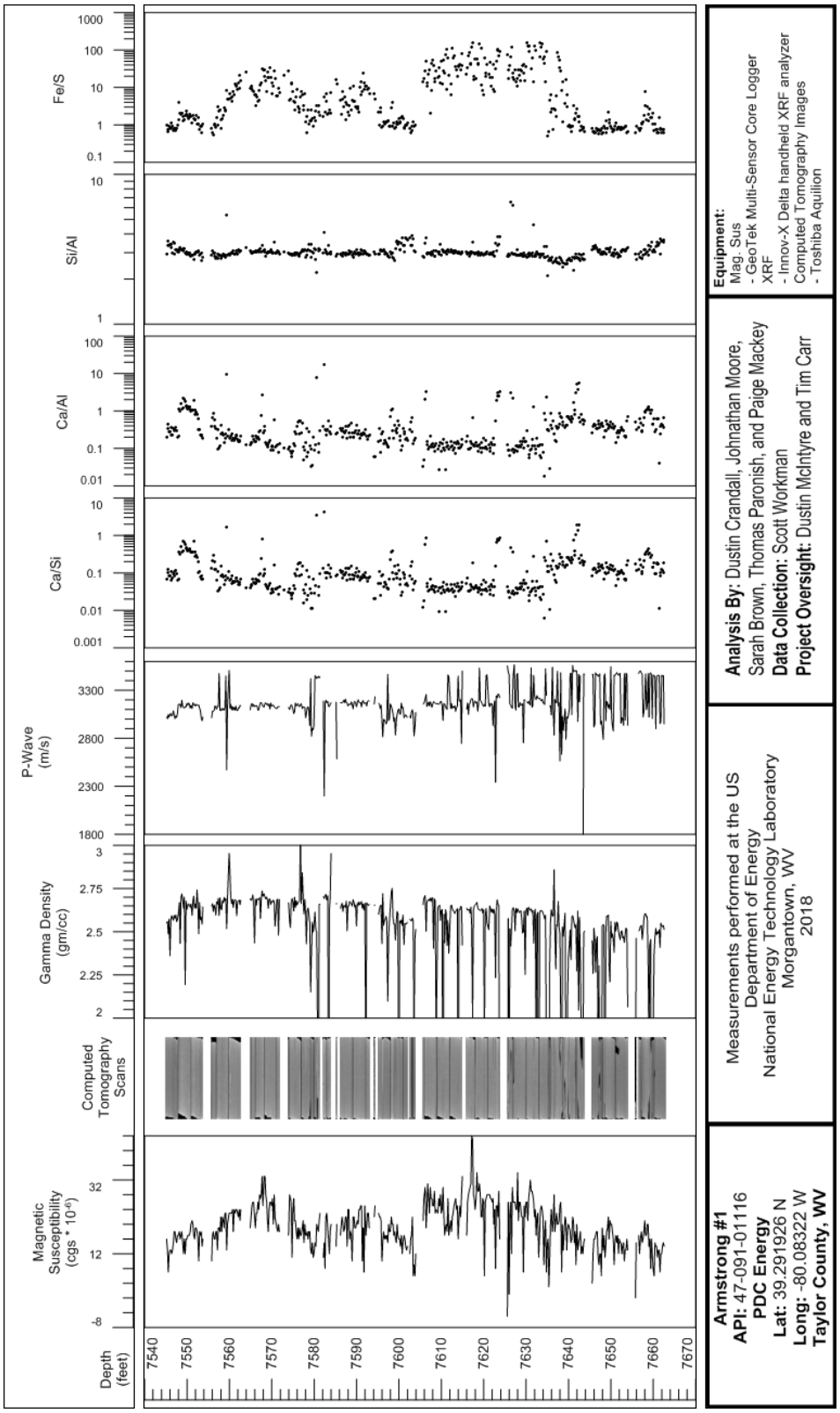

Figure 42: Compiled core log with elemental ratios, and detailed core description for Armstrong #1, from 7,545 to 7,662.5 ft.

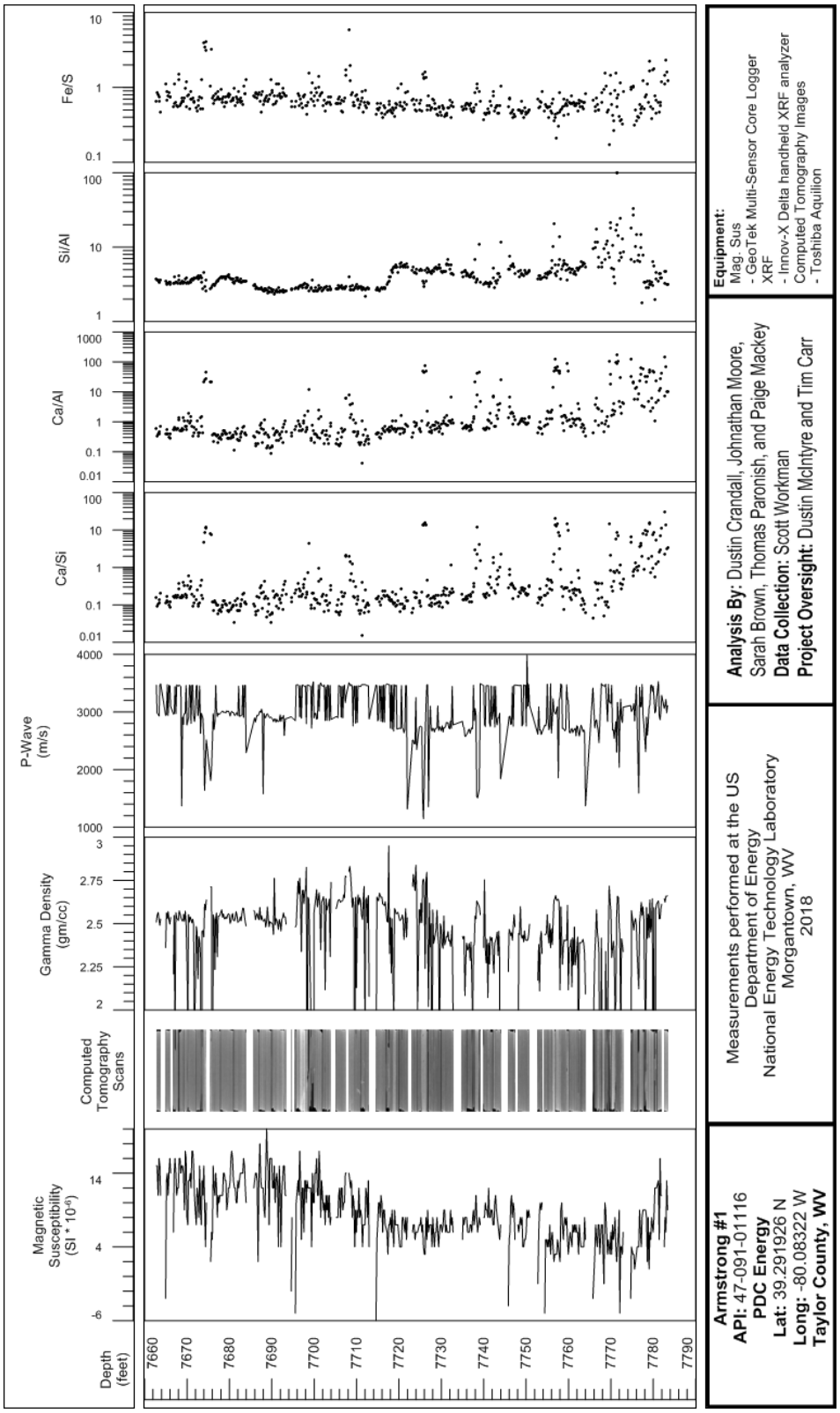

Figure 43: Compiled core log with elemental ratios, and detailed core description for Armstrong #1, from 7,662.5 to 7,783.4 ft.

5. DISCUSSION

The measurements of the magnetic susceptibility, P-wave velocity, XRF, and CT analysis provide a unique look into of the internal structure of the core and macroscopic changes in lithology. These techniques:

- Are non-destructive
- When performed in parallel, give insight into the core beyond what one individual technique can provide
- Can be used to identify zones of interest for detailed analysis, experimentation, and quantification
- Provide a detailed digital record of the core, before any destructive testing or further degradation, that is accessible and can be referenced for future studies.

This page intentionally left blank.

6. REFERENCES

Cnudde, V.; Boone, M. N. High-resolution X-ray computed tomography in geosciences: A review of the current technology. *Earth-Science Reviews* **2013,** *123*, 1–17.

Crandall, D.; Paronish, T.; Brown, S.; Martin, K.; Moore, J.; Carr, T. R.; Panetta, B. *CT Scanning and Geophysical Measurements of the Marcellus Formation from the Tippens 6HS Well;* NETL-TRS-3-2018; NETL Technical Report Series; U.S. Department of Energy, National Energy Technology Laboratory: Morgantown, WV, 2018a; p 32.

Crandall, D.; Moore, J.; Brown, S.; Martin, K.; Mackey, P.; Paronish, T.; Carr, T.; Bowers, C. *Computed Tomography Scanning and Geophysical Measurements of Core from the Coldstream 1MH Well*; NETL-TRS-5-2018; NETL Technical Report Series; U.S. Department of Energy, National Energy Technology Laboratory: Morgantown, WV, 2018b; p 48.

Crandall, D.; Moore, J.; Rodriguez, R.; Gill, M.; Soeder, D.; McIntyre, D.; Brown, S. *Characterization of Martinsburg Formation using Computed Tomography and Geophysical Logging Techniques*; NETL-TRS-4-2017; NETL Technical Report Series; U.S. Department of Energy, National Energy Technology Laboratory: Morgantown, WV, 2017; p 68.

Energy Information Administration (EIA), shapefiles. https://www.eia.gov/maps/maps.htm#shaleplay (accessed Jan 2018).

Geotek Ltd. Geotek Multi-Sensor Core Logger Flyer, Daventry, UK, 2009. http://www.geotek.co.uk/sites/default/files/MSCLOverview.pdf

Geotek Ltd. Multi-Sensor Core Logger Manual; Version 05-10; Published by Geotek, 3 Faraday Close, Daventry, Northamptonshire NN11 8RD, 2010. info@geotek.co.uk, www.geotek.co.uk

Rasband, W. S. ImageJ. U.S. National Institutes of Health: Bethesda, MD, 1997–2016, http://imagej.nih.gov/ij/ (accessed 2018).

This page intentionally left blank.

Sean Plasynski, Ph.D.
Director (Acting)
National Energy Technology Laboratory
U.S. Department of Energy

Jared Ciferno
Associate Director
Oil and Gas
Technology Development & Integration Center
National Energy Technology Laboratory
U.S. Department of Energy

Elena Melchert
Director
Division of Upstream Oil and Gas Research
U.S. Department of Energy

Bryan Morreale
Executive Director
Research and Innovation Center
National Energy Technology Laboratory
U.S. Department of Energy

NETL Technical Report Series